Received: 12 February 2021 | Revised: 10 April 2021 | Accepted: 19 May 2021

DOI: 10.1002/hipo.23366

RESEARCH ARTICLE

WILEY

Nitrergic modulation of neuronal excitability in the mouse hippocampus is mediated via regulation of Kv2 and voltage-gated sodium channels

Hannah Scheiblich[1] | Joern R. Steinert[2]

[1]Department of Neurodegenerative Disease and Geriatric Psychiatry/Neurology, University of Bonn Medical Center, Bonn, Germany

[2]Faculty of Medicine and Health Sciences, University of Nottingham, School of Life Sciences, Queen's Medical Centre, Nottingham, UK

Correspondence
Joern R. Steinert, Faculty of Medicine and Health Sciences, University of Nottingham, School of Life Sciences, Queen's Medical Centre, Nottingham, UK.
Email: joern.steinert@nottingham.ac.uk

Funding information
Medical Research Council, Grant/Award Number: MC_U132681855

Abstract

Regulation of neuronal activity is a necessity for communication and information transmission. Many regulatory processes which have been studied provide a complex picture of how neurons can respond to permanently changing functional requirements. One such activity-dependent mechanism involves signaling mediated by nitric oxide (NO). Within the brain, NO is generated in response to neuronal NO synthase (nNOS) activation but NO-dependent pathways regulating neuronal excitability in the hippocampus remain to be fully elucidated. This study was set out to systematically assess the effects of NO on ion channel activities and intrinsic excitabilities of pyramidal neurons within the CA1 region of the mouse hippocampus. We characterized whole-cell potassium and sodium currents, both involved in action potential (AP) shaping and propagation and determined NO-mediated changes in excitabilities and AP waveforms. Our data describe a novel signaling by which NO, in a cGMP-independent manner, suppresses voltage-gated Kv2 potassium and voltage-gated sodium channel activities, thereby widening AP waveforms and reducing depolarization-induced AP firing rates. Our data show that glutathione, which possesses denitrosylating activity, is sufficient to prevent the observed nitrergic effects on potassium and sodium channels, whereas inhibition of cGMP signaling is also sufficient to abolish NO modulation of sodium currents. We propose that NO suppresses both ion channel activities via redox signaling and that an additional cGMP-mediated component is required to exert effects on sodium currents. Both mechanisms result in a dampened excitability and firing ability providing new data on nitrergic activities in the context of activity-dependent regulation of neuronal function following nNOS activation.

KEYWORDS
excitability, hippocampus, nitric oxide, redox signaling, voltage-gated potassium channel, voltage-gated sodium channel

1 | INTRODUCTION

Regulation of neuronal intrinsic excitability is an essential mechanism in adapting neuronal function to continuously changing requirements for reliable information transmission. Many activity-dependent mechanisms have been reported in various neuronal cell types and networks where homeostatic control of network activity can occur via multiple signaling pathways. One example includes changes in synaptic strength, a phenomenon termed "synaptic scaling" (Turrigiano, 1999) with underlying key mechanisms include changes in (i) synaptic activity-driven calcium signaling via glutamate receptor activation, (ii) voltage-gated calcium entry, or (iii) potassium conductances (Brickley et al., 2001; O'Leary et al., 2010). Following calcium influx, an important cascade is triggered, namely the activation of calcium/calmodulin-dependent neuronal nitric oxide (NO) synthase (nNOS). Resulting NO production activates broad signaling, including the NO-induced activation of the canonical cGMP pathway mediated by cGMP generation, activation of protein kinase G (PKG) and associated downstream phosphorylation events. In addition, NO induces the direct posttranslational protein modifications S-nitrosylation (a nonenzymatic reversible reaction of NO^- with cysteine residues) and 3-nitrotyrosination (an irreversible reaction of a tyrosine residue with NO_2). These effects have been widely reported under physiological and neuropathological conditions (Akhtar et al., 2012; Lipton et al., 1994). Both redox-sensitive modifications impact on protein function and thus are essential regulators of neuronal activity in health and disease (Balez & Ooi, 2016; Bradley & Steinert, 2016; Garthwaite, 2019; Steinert, Chernova, & Forsythe, 2010). Modulation by NO has been reported for various ion channels, including voltage-gated potassium channels (Kv), the M-current (Kv7), calcium, sodium, and TRP channels (Gamper & Ooi, 2015). Suppression of Kv3 currents in CHO cells is mediated via cGMP production and phosphorylation (Moreno et al., 2001) and cGMP-mediated suppression of native Kv3.1 currents was shown in principal neurons of the medial nucleus of the trapezoid body (MNTB) (Steinert et al., 2008). L-type calcium channels are inhibited by NO in a cGMP-dependent manner in myofibroblasts (Bae et al., 2020) but augmented in principal neurons of MNTB (Tozer et al., 2012).

It has been long established that nNOS is expressed in hippocampal GABAergic nonprincipal neurons (Jinno et al., 1999; Megias et al., 1997) with a relatively large subpopulation (approximately 30%) of hippocampal parvalbumin- and neuropeptide Y-positive GABAergic interneurons being nNOS positive (Jinno et al., 1999; Tricoire et al., 2010). In addition to regional difference in nNOS expression, functional NO release across hippocampal regions differs greatly (Lourenco, Ferreira, et al., 2014) indicating the diversity of NO production and bioactivity.

Despite published work on activity-dependent homeostasis and modulation of intrinsic excitability, a comprehensive understanding of the mechanisms initiated by NO on neuronal properties is currently lacking due to the diversity of experimental preparations and applications of NO (−donors).

Given the importance and complexity of the nitrergic signaling route, this study was set out to characterize the effects of NO on ion channel activities and excitabilities in native pyramidal neurons within the CA1 hippocampal region by a defined concentration of NO to allow a systematic assessment of nitrergic effects. CA1 pyramidal neurons possess a range of Kv channels. The main determinants in shaping the action potential (AP) waveform and regulating excitabilities are potassium channels belonging to the families of high-voltage gated Kv3 (mainly Kv3.1 and Kv3.2) and Kv2 "delayed-rectifier" channels, with Kv2.1 being the predominant Kv channel expressed in pyramidal neurons (Kirizs et al., 2014). Low voltage-activated Kv1 channels are involved in setting AP thresholds (Jan & Jan, 2012) and voltage-gated sodium channels (Na_v), once activated, are responsible for the depolarizing upstroke and amplitude of an AP (Bean, 2007). The most prominent members of the Na_v family in hippocampal pyramidal neurons are the $Na_v1.2$ and $Na_v1.6$ (Westenbroek et al., 1989). In addition, there are several potassium channels possessing a more regulatory function which are activated around resting membrane potentials, such as the hyperpolarization-activated cyclic nucleotide-gated ion channel (HCN) or the M-current (belonging to the subthreshold-active Kv7 family of potassium channels). For instance, Kv7.2/Kv7.3 channels stabilize the membrane potential and increase Na_v channel availability and AP amplitudes (see review Trimmer, 2015).

In this study, we assessed the main elements of information transmission in native CA1 pyramidal neurons, for example, AP firing and neuronal excitability, which are predominantly regulated by Kv2 and voltage-gated sodium channels. We characterized the involvement of cGMP- and redox-sensitive signaling by applying voltage protocols which specifically assess high voltage-activated Kv3, Kv2 as well as Na_v activities and exclude HCN or Kv4 (A-current [Kv4.2, Kv4.3]) channels, and, in combination with specific pharmacology, separated Kv3 and Kv2 currents. We found that Kv2 potassium channels were suppressed via a cGMP-independent and reversible redox-sensitive pathway, suggesting the involvement of S-nitrosylation. Sodium channel activities were suppressed by NO, requiring both, a cGMP-dependent and redox-sensitive component, indicating combined and possibly additive phosphorylation and S-nitrosylation mechanisms. Effects on both ion channels led to a widening of AP waveforms and reduction in firing rates of pyramidal neurons.

2 | METHODS

2.1 | Study approval

All animal work conformed to the United Kingdom Home Office regulations. All procedures (both nonregulated and regulated) were conducted under a Home Office project license awarded to Joern Steinert under the Animals (Scientific Procedures) Act 1986.

2.2 | In vitro brain slice preparations

C57/BL6 mice aged P14–P22 were killed by decapitation and slices containing the hippocampus were prepared as previously described

(Steinert et al., 2011). Data were generated from 28 female mice with 3–4 brain slices per mouse and 3–8 neurons per slice. Horizontal slices (200 μm thick) were cut in a low-sodium artificial CSF (aCSF) at ~0°C. Slices were maintained in a normal aCSF at 37°C for 1 h, after which they were stored at room temperature (~20°C). Composition of the normal aCSF was (in mM) as follows: NaCl 125, KCl 2.5, $NaHCO_3$ 26, glucose 10, NaH_2PO_4 1.25, sodium pyruvate 2, myo-inositol 3, $CaCl_2$ 2, $MgCl_2$ 1, and ascorbic acid 0.5; L-arginine 0.1; pH was 7.4, bubbled with 95% O_2, 5% CO_2. For the low-sodium aCSF, NaCl was replaced by 250 mM sucrose, and $CaCl_2$ and $MgCl_2$ concentrations were changed to 0.1 and 4 mM, respectively. Osmolarity was adjusted to 310 mosmol/L.

2.3 | Electrophysiology

Whole-cell patch recordings were made from pyramidal neurons visually identified in the mid-third CA1 region in acute brain slices of the hippocampus as described previously (Bradley et al., 2017). Patch pipettes were pulled from glass capillaries (GC150F-7.5, o.d. 1.5 mm, Harvard Apparatus, Edenbridge, UK) with resistances of 3–5 MΩ. Series resistances (R_s) were between 7 and 15 MΩ (R_s compensation and prediction were set to 75–85%, electrode and whole-cell capacitance were compensated). Data were obtained using a Multiclamp 700B amplifier and Digidata 1550 ADDA converter. Acquisition (20 kHz sampling rate) and analysis were performed using pClamp 10.4 (Molecular Devices, Sunnyvale, CA). In current clamp, the amplifier circuitry was used to compensate the bridge balance (with pipette capacitance fully neutralized) and for experiments involving measurements of AP firing, current was injected to hold the membrane potential at −60 mV. AP firing threshold was defined as the point of maximum curvature of the voltage waveform between the onset of stimulation and the spike maximum at rheobase (Sekerli et al., 2004).

The pipette solution for whole-cell recordings contained 120 mM potassium gluconate, 10 mM HEPES, 0.2 mM EGTA, 4 mM K-ATP, 0.3 mM Na-GTP, 10 mM KCl, 8 mM NaCl, pH 7.4 with osmolarity set between 280 and 290 mosmol/L. All experiments were carried out at 33 ± 1°C using feedback control of a Peltier device warming the perfusing aCSF (1 ml/min).

In voltage-clamp, holding potentials were −60 mV and following a hyperpolarizing prepulse to −90 mV (360 ms) and additional prestep to −40 mV (35 ms), voltage command steps ranged from −110 to +50 mV (100 ms) to record voltage-activated potassium currents (Kv). The prestep to −90 mV removed steady-state inactivation of Kv channels and the prestep to −40 mV induced inactivation of Kv4 currents and voltage-gated sodium currents to isolate high-voltage activate Kv2 and Kv3 conductances (Choudhury et al., 2020). The recorded potassium currents generated current–voltage (I–V) relationships (current measures were taken at a latency of 20 ms of the depolarizing step). Activation curves were fitted by the Boltzmann equation: $\frac{I}{Imax} = \frac{1}{1+e^{\left[\frac{V-Vhalf}{k}\right]}}$, where I is the tail current recorded at 0 mV after a prestep to command potential V (currents were estimated from the amplitudes of exponentials backfitted to the beginning of the test step), V_{half} ($V_{1/2}$) is the membrane potential at which I is equal to one-half I_{max} and k is the slope factor. APs were evoked in current clamp by 12.5 pA-step current injections ranging from 0 to +200 pA for constructing current input–output relationships. All AP properties were determined from the first AP elicited at rheobase. To illustrate AP dynamics between groups, the changes in AP waveforms were demonstrated by generating phase plots. Input resistances (R_{in}) were determined according to Ohm's law by measuring the steady-state voltage deflection generated by 50 pA hyperpolarizing current injection for a 180 ms duration. Then, 50 pA of hyperpolarizing current was chosen because such a current intensity minimized the potential sag (Zemankovics et al., 2010). The membrane time constant (τ) was calculated by fitting a single exponential curve to the charging trajectory of the membrane potential between 10 and 90%, see Table 1 for passive membrane properties.

Sodium current steady-state voltage dependent inactivation was determined by a voltage protocol consisting of a 500 ms prepulse to potentials ranging from −90 to −15 mV (V, prepulse potential) followed by a 100 ms test pulse to −30 mV. Peak sodium currents were measured at a latency between 0.5 and 1.5 ms. The steady-state inactivation curves were constructed from currents activated at the corresponding prepulse potential (V) fitted to the Boltzmann function: $\frac{I}{Imax} = \frac{1}{1+e^{\left[\frac{V-Vhalf}{k}\right]}}$. To minimize space clamp errors in nonspherical CA1 pyramidal neurons, we excluded recordings with R_s > 10 MΩ and cell capacitance above 150 pF. In addition, we reduced current amplitudes by measuring at half-maximal channel activation (−30 mV) and excluded sodium current recordings which showed current activation with substantial delays, which would be a characteristic of the activation of channels in neurites (axon and dendrite) that are not adequately voltage-clamped (Cummins et al., 2009).

All R_S within and between data sets were indifferent (p > .05, one-way analysis of variance [ANOVA]). In cells with larger potassium currents activated by stronger depolarizations (+50 mV), the remaining noncompensated R_S can potentially lead to errors in voltages seen by the membrane. One way to minimize such voltage

TABLE 1 Intrinsic membrane properties of pyramidal CA1 neurons (R_{in}: input resistance, C_{mem}: membrane capacitance, τ_{mem}: membrane time constant)

	Ctrl	NOC 5 min	NOC 10 min	NOC 20 min	NOC 30 min	NOC 50 min	*p*-Value
R_{in} (MΩ)	172.2 ± 12.4	205.4 ± 10.5	151.8 ± 15.7	174.6 ± 15.5	213.4 ± 25.1	185.8 ± 20.3	.066
C_{mem} (pF)	94.1 ± 10.1	91.0 ± 8.1	109.1 ± 11.1	101.5 ± 12.6	75.3 ± 6.5	96.1 ± 21.0	.446
τ_{mem} (ms)	15.6 ± 1.4	17.7 ± 2.2	15.8 ± 1.6	16.9 ± 1.8	14.8 ± 1.8	15.8 ± 1.7	.905

clamping errors is to record smaller currents. As such, in Figure 1(b), we compared in addition to currents measured at +50 mV (~10 nA) also currents at 0 mV (~2–3 nA). Currents at both voltages revealed identical changes under the test conditions (NOC-5 application). We therefore focused in subsequent figures on Kv currents measured at +50 mV. All data points are from unpaired experiments and recorded at indicated time points of drug exposure with each data set having its own controls. Voltages were not corrected for liquid junction potentials.

2.4 | Drug application

Drugs were applied by addition to the aCSF perfusing the recording chamber at time 0 min unless otherwise stated: 1H-[1,2,4]oxadiazolo [4,3,-a]quinoxalin-1-one (ODQ, 10 μM); 3-isobutyl-1-methylxanthine (IBMX 10 μM); 8-bromo-cyclic GMP (8-Br-cGMP, 10 μM); glutathione ethyl-ester (GSH, 1 mM); 3-(5′-hydroxymethyl-2′-furyl)-1-benzyl-indazole (YC-1, 10 μM); tetraethylammonium (TEA, 1 mM); Guangxitoxin-1E (GxTx-1E, 100 nM); 3-(aminopropyl)-1-hydroxy-3-isopropyl-2-oxo-1-triazene (NOC-5, 10 μM).

2.5 | Statistical analysis

Results are expressed as the means ± *SEM*. Statistical comparisons were made by one-way ANOVA with Newman–Keuls posteriori analysis, two-way ANOVA with Bonferroni's multiple comparisons test, as appropriate. All data sets were tested for normality using the Shapiro–Wilk test showing normal data distributions. A *p*-value smaller than .05 was considered as significant. Asterisks directly above bars indicate *p*-values relative to corresponding controls, each data set has its own controls. Significance between other conditions is indicated by a line above the bars. All statistical tests were performed using GraphPad Prism 9 software.

3 | RESULTS

3.1 | NO suppresses voltage-gated potassium currents

Divergent physiological phenotypes have been reported in response to NO applications or endogenous release due to the complexity of its downstream signaling. We decided to investigate the effects of NO in intact native pyramidal CA1 neurons allowing the required physiological signaling to occur. We first wanted to address how NO, delivered by a NO donor (NOC-5, 10 μM, equal to ~400–500 nM of released NO (Bradley & Steinert, 2015)), affects voltage-gated potassium currents (Kv) in CA1 pyramidal neurons over a time window of up to 50 min. Whole-cell I–V curves of individual neurons were constructed between −110 to +50 mV at 5, 10, 20, 30, and 50 min timepoints of NOC-5 exposure. The different time points were chosen as the nature of nitrergic effects may differ depending on its downstream signaling and exposure time. Furthermore, to avoid dialysis of any endogenous signaling molecules, whole-cell recordings performed at the indicated timepoints did not last longer than 2–3 min and data are presented as unpaired results. Example raw traces and I–V curves are shown in Figure 1(a) with NO suppressing outward currents between 0 and +50 mV at 5 and 30 min (Figure 1(a), Ctrl vs. NOC: 0 mV@30 min: $p = .0013$; between +10 and +50 mV@both timepoints: $p < .0001$, two-way ANOVA). Comparing outward currents at +50 mV shows that NO suppressed currents between 5 and 50 min (Figure 1(b), Ctrl vs. NOC: $p = .0004$ @5 min; $p = .0051$ @10 min, $p = .0031$ @20 min, $p = .0003$ @30 min, $p = .0264$ @50 min, one-way ANOVA). Passive intrinsic membrane properties were not affected by NO (Table 1). Although R_s values were indifferent between test conditions, larger currents can cause voltage clamping errors. In order to lessen those potential errors, we also compared smaller currents at 0 mV, typically around 2–3 nA, and found that NO similarly suppressed current amplitudes at this voltage following 20 min of exposure (Figure 1(b), lower graph, Ctrl vs. NOC: $p = .0101$ @20 min; $p = .0072$ @30 min, $p = .0223$ @50 min, one-way ANOVA). Next, we wanted to elucidate the signaling routes by which NO exerts its effects. First, we exposed slices to NOC-5 in the presence of 10 μM ODQ (with 10 min pre-incubation) to block the activation of the endogenous NO receptor soluble guanylyl cyclase (sGC) that synthesizes cGMP from GTP (IC_{50} for sGC: ~1 μM (Garthwaite et al., 1995)). Inhibition of sGC did not preclude the NO-mediated reduction of Kv currents suggesting that the nitrergic effects are not caused via the canonical cGMP pathway but rather a NO-mediated posttranslational modification which could be caused by either a reversible S-nitrosylation or irreversible 3-nitrotyrosination modification (Figure 1(c), raw traces and I–V curves, Ctrl vs. 30 min NOC + ODQ: $p = .0086$ @20 mV, $p < .0001$ @30–50 mV, wash out vs. 30 min NOC + ODQ: $p = .0292$ @40 mV, $p = .0046$ @50 mV, Ctrl vs. wash out: $p > .05$, two-way ANOVA; Figure 1(d), Ctrl vs. NOC + ODQ: $p = .0326$ @10 min; $p = .0016$ @20 min and $p = .0057$ @30 min, one-way ANOVA). Testing for reversibility of the current suppression would distinguishing between both posttranslational modifications. We recorded from neurons at 25 min (washout in NO-free aCSF) after NO exposure for 50 min. These data show that currents recorded from neurons which were exposed for 50 min to NO followed by a 25 min NO-free aCSF washout remained unaltered, suggesting a reversible current modulation (Figure 1(d), $p = .5521$ @washout, one-way ANOVA). To further support the notion of a cGMP-independent mechanism, we specifically confirmed that pharmacological activation of this pathway *per se* had no effect on outward currents. We recorded currents following incubation with an activator of sGC (YC-1) between 5 and 30 min (Wu et al., 1995), while simultaneously blocking the degradation of cGMP by phosphodiesterases (IBMX) resulting in maximally activated cGMP production (Friebe et al., 1998). Activation of sGC-cGMP signaling did not alter current amplitudes at any time point tested (Figure 1(e), Ctrl vs. YC-1 + IBMX: $p = .818$ @10 min, $p = .242$ @20 min, $p = .399$ @30 min; Ctrl vs. NOC 5–50 min [average data taken from Figure 1(b) for comparison]: $p = .0022$, one-way ANOVA)

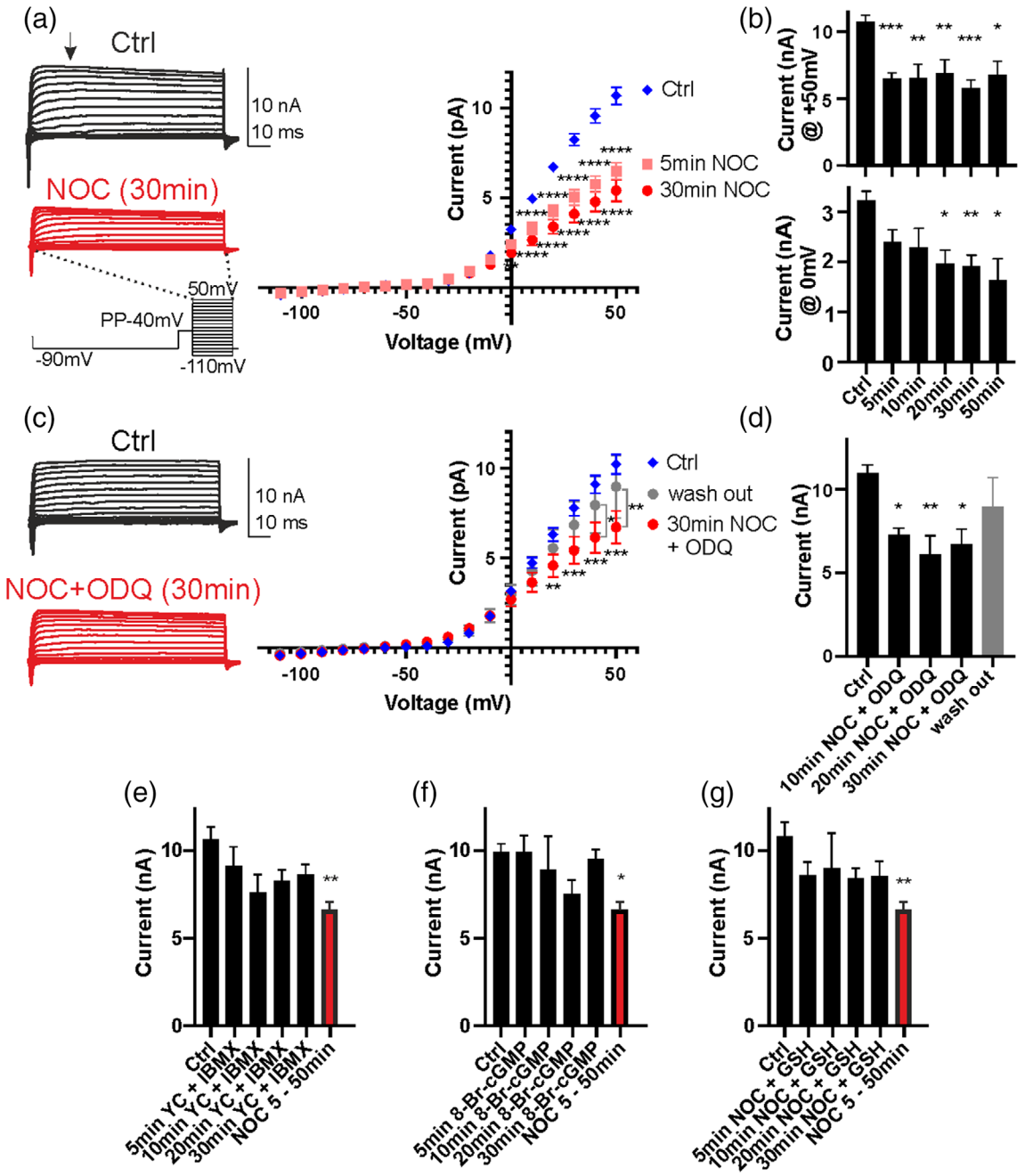

FIGURE 1 Nitric oxide (NO)-mediated suppression of high-voltage activated potassium currents in CA1 pyramidal neurons is cGMP-independent but redox sensitive. (a) Left, sample voltage-clamp recordings from a control and NO-treated neuron (10 μM NOC-5) with voltage protocol below (arrow indicates latency at which current was measured). Right, summary IV curves for two timepoints: NO treatment reduced outward currents after 5 min at voltages positive to +10 mV and after 30 min at voltages positive to 0 mV (5 min NOC vs. Ctrl and 30 min NOC vs. Ctrl, two-way ANOVA). (b) Summary of mean current amplitudes at +50 and 0 mV. (c) Left, sample recordings from a control and NOC + ODQ-treated neuron. Right, summary IV curves for control and treated neurons: NOC + ODQ treatment suppresses outward currents between 20 and 50 mV (wash out vs. Ctrl: $p > .05$ and wash out vs. NOC + ODQ at 40 and 50 mV: $p < .05$). (d) Summary of mean current amplitudes at +50 mV. (e) Summary of mean current amplitudes at 50 mV at indicated timepoints following incubation with YC-1 (10 μM) + IBMX (10 μM), 5–50 min NOC data are average data taken from (c) for comparison. (f) Summary of mean current amplitudes at 50 mV at indicated timepoints following incubation with 8-Br-cGMP (10 μM), 5–50 min NOC data are average data taken from (c). (g) Summary of mean current amplitudes at 50 mV at indicated timepoints following incubation with NOC-5 (10 μM) + glutathione (GSH, 1 mM), 5–50 min NOC data are average data taken from (c) for comparison. Data denote mean ± *SEM* ($n = 6$–14 cells). Significance tested by two-way analysis of variance (ANOVA) (a,c) and one-way ANOVA (b,d,e–g) with $^{*}p < .05$, $^{**}p < .01$, $^{***}p < .001$, $^{****}p < .0001$

confirming that cGMP signaling is not involved in the observed nitrergic effects. Complementary experiments to activate PKG directly by 10 μM 8-Br-cGMP, a nonhydrolysable analogue of cGMP (Lu & Hawkins, 2002), also failed to alter whole-cell currents (Figure 1(f), Ctrl vs. 8-Br-cGMP: $p > .05$ @ any time point, Ctrl vs. NOC 5–50 min [NOC average data taken from Figure 1(b) for comparison]: $p = .034$, one-way ANOVA).

We concluded that cGMP and PKG activation are unlikely to be responsible for the nitrergic effects on outward currents and that the mechanism to regulate ion channel protein function may be via NO-induced reversible S-nitrosylation. We next tested whether suppressing the redox-sensitive S-nitrosylation impacts on the effects caused by NO by incubating the slices with membrane permeable GSH prior to (20 min) and during NO exposure. GSH has a strong reducing capacity and is the main cellular reactant to prevent cysteine S-nitrosylation (Clementi et al., 1998; Stomberski et al., 2019). Incubation with 1 mM GSH prevented the nitrergic effects on Kv currents, although a nonsignificant tendency to smaller currents remained (Figure 1(g), Ctrl vs. NOC + GSH [@ any timepoint]: $p > .05$, Ctrl vs. NOC 5–50 min [NOC average data taken from Figure 1(b) for comparison]: $p = .0052$, one-way ANOVA). The data therefore imply a nitrergic redox-sensitive reaction as the underlying cause for current reductions.

Having established nitrergic effects on whole-cell potassium currents we wanted to characterize the underlying affected conductances. CA1 pyramidal neurons express high levels of voltage-gated Kv2 channels (Kv2.2 and Kv2.1) (Kirizs et al., 2014; Mohapatra et al., 2009; Palacio et al., 2017) and only a subset of the pyramidal neurons (~17%) expresses Kv3.1 and Kv3.2 channels, with fast-spiking interneurons being the main source of Kv3 conductances in the hippocampus (Du et al., 1996; Martina et al., 1998). To determine which of the channels is affected by nitrergic GSH-dependent modulation, we used the Kv3 channel blocker, TEA, at a concentration of 1 mM to specifically eliminate Kv3 (Coetzee et al., 1999). Incubation with 1 mM TEA blocked ~10% of total outward currents only at +50 mV (Figure 2(a), $p = .0069$, two-way ANOVA). However, additional exposure to NO further diminished the remaining currents between +10 and +50 mV (Figure 2(a), $p < .05$, two-way ANOVA). Mean data at +50 mV are summarized in Figure 2(c) (Ctrl vs. TEA: $p = .2154$; Ctrl vs. TEA + NOC: $p < .0001$, TEA vs. TEA + NOC: $p = .0175$, TEA vs. NOC 5–50 min: $p < .0001$ [NOC 5–50 min average data taken from Figure 1(b)], one-way ANOVA) suggesting that the observed effects of NO were not mediated by Kv3 modulation. Maximizing cGMP production by YC-1 + IBMX incubation in the presence of TEA did not impact on TEA-insensitive currents (Figure 2(c), $p > .05$, one-way ANOVA). Next, we tested whether Kv2 currents were a potential target for NO and used 100 nM GxTx-1E which exhibits high potency for blockade of Kv2 (Lee et al., 2010). Following inhibition of Kv2 currents (Figure 2(b), +20 to +50 mV: $p < .0001$, two-way ANOVA) we did not observe any further decline in currents after additional NO exposure (Figure 2(b), GxTx-1E vs. GxTx-1E + NOC: $p > .05$, two-way ANOVA; Figure 2(c), Ctrl vs. GxTx-1E: $p = .0048$, Ctrl vs. GxTx-1E + NOC: $p = .0263$; GxTx-1E vs. GxTx-1E + NOC: $p = .99$, Ctrl vs. NOC 5–50 min: $p < .0001$ [NOC 5–50 min average data taken from Figure 1(b)], one-way ANOVA). Activation of the cGMP-PKG cascade following GxTx-1E application did not further impact on the current amplitudes (GxTx-1E vs. GxTx-1E + YC-1 + IBMX: $p > .05$, one-way ANOVA). All recordings were performed using a prepulse protocol (step to −40 mV) to inactivate Kv4 (A-type) channels thereby excluding this channel contributing to the observed nitrergic effects on whole-cell outward currents. Taking together, these data show that Kv3 is not modulated by NO, however, since in the absence of Kv2 (+GxTx-1E), we do not see any NO-induced changes in currents; our data imply that Kv2 is the main target underlying the observed nitrergic effects.

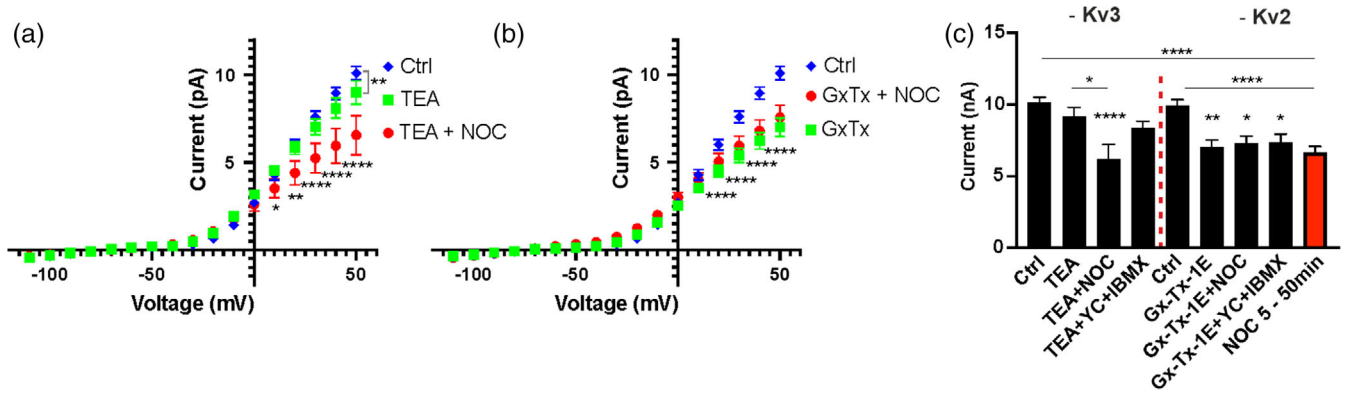

FIGURE 2 GxTx-1 but not tetraethylammonium (TEA) prevents nitrergic effects on potassium currents. (a) Summary IV curves for control neurons and neurons treated with TEA and TEA + NOC at a 30 min timepoint. TEA only reduced outward currents at 50 mV (TEA vs. Ctrl: @50 mV: $p = .0069$, two-way analysis of variance [ANOVA]), addition of NO leads to substantial reduction of currents between 10 and 50 mV (TEA vs. TEA + NOC: @10 mV: $p = .0419$, @20 mV $p = .0023$, @30 to 50 mV: $p < .0001$, two-way ANOVA). (b) Summary IV curves for control neurons and neurons treated with GxTx-1 and GxTx-1 + NOC at a 30 min timepoint. GxTx-1 reduces outward currents between 20 and 50 mV (GxTX-1 vs. Ctrl: each voltage: $p < .0001$, two-way ANOVA) with nitric oxide (NO) treatment having no further effects (each voltage: $p > .05$). (c) Summary of mean current amplitudes at 50 mV at 30 min exposure. Data denote mean ± *SEM* ($n = 8$–18 cells). Significance tested by two-way ANOVA (a,b) and one-way ANOVA (c) with $^{*}p < .05$, $^{**}p < .01$, $^{****}p < .0001$

If NO modulates a specific subset of outward currents we would predict that half-activation voltages ($V_{1/2}$) of the remaining currents may change, as different voltage-gated currents differ in their activation voltage range (Du et al., 2000; Lien et al., 2002; Martina et al., 1998). Furthermore, activation kinetics change in response to differential channel clustering and posttranslational modifications as reported for Kv2 (Du et al., 2000; Misonou et al., 2004; Mohapatra et al., 2009). To determine $V_{1/2}$ values we measured tail current amplitudes over an activation range from −70 to +70 mV (Figure 3(a)) and fitted a Boltzmann function to the relative current amplitudes. Fitted curves for controls and following NO application are shown in Figure 3(b) (top). $V_{1/2}$ values in control neurons were in the range of 0 to +5 mV (Figure 3(b), bottom) as reported previously for pyramidal CA1 neurons (Mohapatra et al., 2009). Interestingly, incubation with NOC-5 caused a hyperpolarizing shift of $V_{1/2}$ to values of around −10 mV (Figure 3(b), bottom, one-way ANOVA). This shift was completely abolished by GSH and unaffected by ODQ (Figure 3(c,d), one-way ANOVA) suggesting that the nitrergic effects on $V_{1/2}$ were directly mediated by NO. Importantly, following NO exposure in the presence of TEA, we saw a hyperpolarizing shift in $V_{1/2}$ relative to TEA alone, and despite being of smaller magnitude (Figure 4(a), one-way ANOVA), the data confirm a modulation of high-voltage-activated currents other than Kv3. However, when blocking Kv2 by GxTx-1E, the NO-induced changes of $V_{1/2}$ were not observed (Figure 4(b), one-way ANOVA), again suggesting a modulation of Kv2 channels. Interestingly, the slope factor (k) was neither affected by TEA nor by NO in the presence of TEA (k_{Ctrl}: 14.3 ± 0.6, k_{TEA}: 15.8 ± 0.5, $k_{TEA+NOC}$: 16.0 ± 1.2, $p > .05$, one-way ANOVA); however, GxTx-1E caused a shift in k which remained unchanged in the presence of NO (k_{Ctrl}: 14.5 ± 0.6, $k_{GxTx\text{-}1E}$: 19.3 ± 1.1 ($p = .005$), $k_{GxTx\text{-}1E+NOC}$: 21.3 ± 1.0 ($p = .0002$), one-way ANOVA). Selective activation of cGMP signaling by YC-1 + IBMX following inhibition of either Kv3 or Kv2 did not impact on the half-activation voltages (Figure 4(a,b), $p > .05$ vs. respective Ctrl, one-way ANOVA) or k values ($p > .05$, one-way ANOVA).

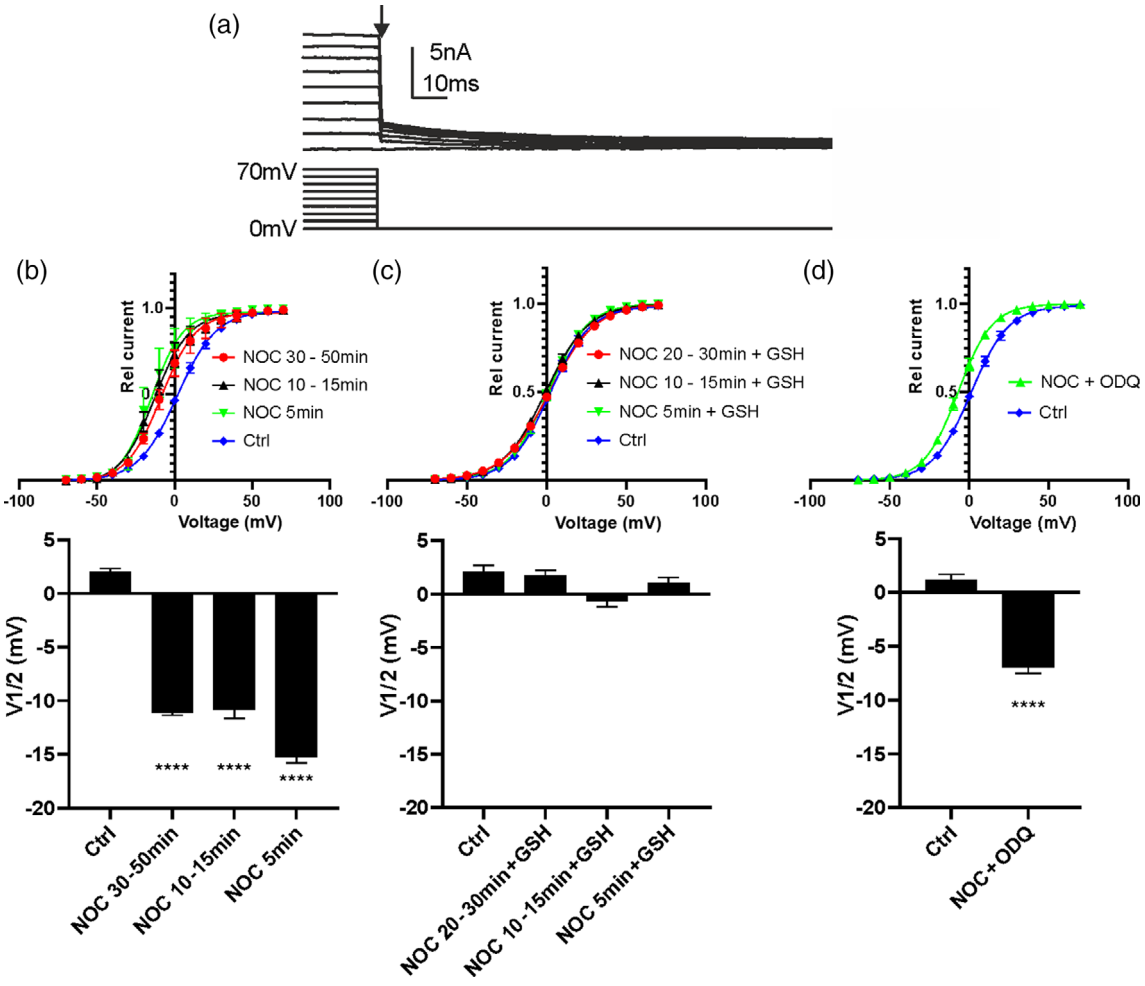

FIGURE 3 Nitric oxide (NO) changes voltage dependence of Kv activation which was prevented by glutathione and unaffected by ODQ. (a) Sample voltage-clamp recording of a tail currents (amplitude measured by exponential fit to time 0, indicated at arrow), below, voltage protocol. (b–d) Top, voltage dependence of current activation under indicated conditions was determined by plotting tail currents at 0 mV as a function of the test voltages. Solid lines represent fit with simple Boltzmann function. (b–d) Bottom, summary $V_{1/2}$ values for indicated conditions. Data denote mean ± *SEM* ($n = 6$–18 cells). Significance tested by one-way analysis of variance (ANOVA) (b,c) and Student's t test (d), ****$p < .0001$

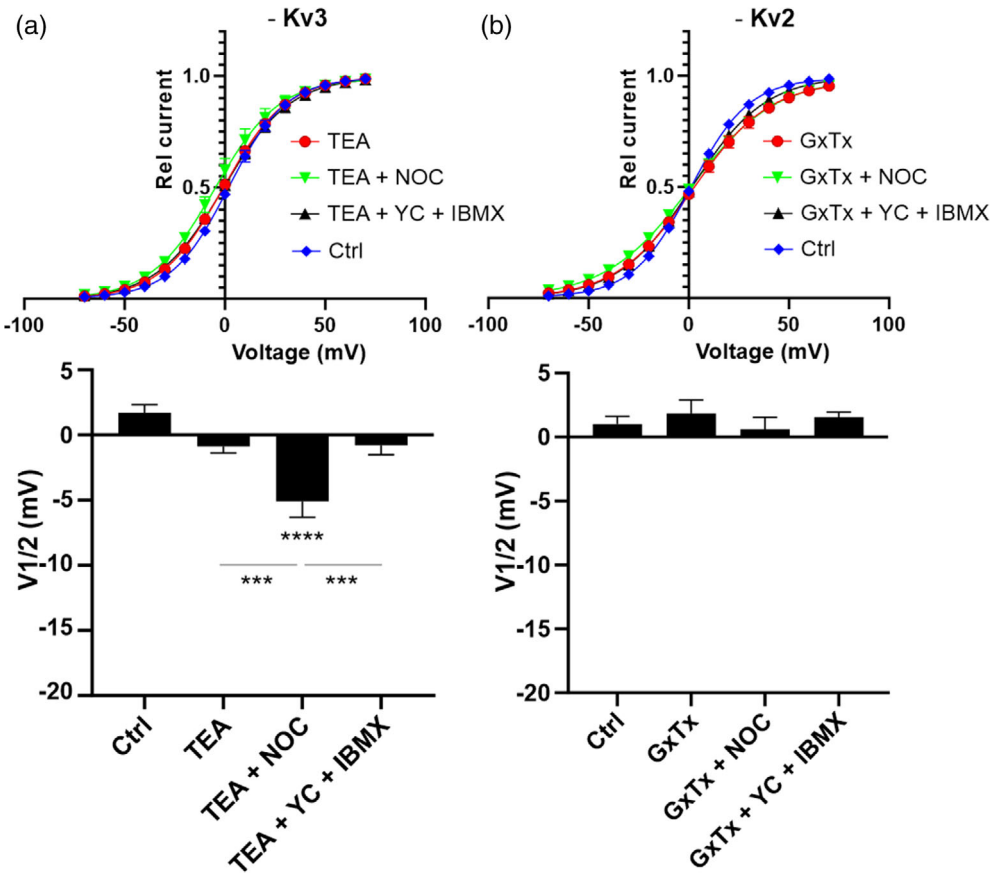

FIGURE 4 Nitric oxide (NO) but not cGMP signaling changes voltage dependence of Kv activation in the presence of tetraethylammonium (TEA) but not in the presence of GxTx-1. (a,b) Top, voltage dependence of current activation under indicated conditions was determined by plotting tail currents at 0 mV as a function of the test voltages. Solid lines represent fit with simple Boltzmann function. (a,b) Bottom, summary $V_{1/2}$ values for indicated conditions. Data denote mean ± *SEM* ($n = 8–18$ cells). Significance tested by one-way analysis of variance (ANOVA) with ***$p < .001$, ****$p < .0001$

3.2 | NO induces wider APs and reduces intrinsic excitability

Having established that NO modulates Kv2 currents, we next wanted to assess the effects of NO on the basic elements of information transmission including the characteristics of an AP and associated neuronal excitabilities. As high voltage-activate potassium currents, in addition to voltage-gated sodium and low voltage-activated potassium currents shape an AP waveform and set firing thresholds, we assessed these different AP parameters (half-width, amplitude and threshold) under various conditions of nitrergic activity. We expected an increase in half-width since the repolarizing phase of an AP in the hippocampus is determined by the strength of Kv2 currents (Liu & Bean, 2014). Indeed, we found that NO exposure over the time course of 5–50 min resulted in a substantial increase in half-widths of depolarization-evoked APs (Figure 5(a,b), half-width of first AP at rheobase: Ctrl vs. NOC: 5 min: $p = .0207$, 10 min: $p = .255$, 20 min: $p = .017$, 30 min: $p = .0172$, 50 min: $p = .0262$, one-way ANOVA). This AP widening will induce a significant effect during prolonged trains of AP firing by enhancing failure rates due to accumulating inactivation of voltage-gated sodium currents. To test this scenario under our conditions we injected increasing levels of depolarizing currents ranging from 0 to 200 pA for 180 ms from a holding voltage of −60 mV and generated input–output relationships. Under control conditions, we recorded an increasing number of APs with stronger current injection (Figure 5(a,c)). Following 5 min of NO exposure the number of APs was reduced at and above 150 pA of current injection (Figure 5(c), green arrow, $p = .011$, two-way ANOVA) reaching highly significant reductions at and above 62.5 pA of current injection after 30 min NO exposure (Figure 5(c), red arrow, $p = .0248$).

Although cGMP signaling itself did not impact on Kv currents, we tested whether AP waveforms were affected by pharmacological modulation of cGMP production. We confirmed that NO exposure in the presence of ODQ led to an increase in AP half-widths (first AP at rheobase), again confirming a cGMP-independent mechanism (Figure 5(d,e), Ctrl vs. NOC + ODQ: 10 min: $p = .0071$, 20 min: $p = .0334$, 30 min: $p = .0422$, one-way ANOVA). Importantly, in the presence of ODQ, NO only reduced the depolarization-evoked firing rates after longer exposure times (>30 min) at and above 125 pA of current injection (Figure 5(f), red arrow, $p = .0176$, two-way ANOVA). Thus, ODQ diminished but not eliminated the effects seen by NO alone. During an AP, the change of the membrane potential is proportional to ionic current flow with the steepest portion during the upstroke occurring at maximal sodium current flow (Liu & Bean, 2014). This parameter can be assessed in phase plots illustrating the change in voltage over time (dV_m/dt). NO application reduces the upstroke of the AP (Figure 5(g)) suggesting diminished sodium current activities. Interestingly, we also noticed a decrease in AP amplitudes after NO incubation between 20 and 30 min (first AP, Figure 5(h), Ctrl vs. NOC: 20 min: $p = .0074$, 30 min: $p = .003$, one-way ANOVA) without changes in firing thresholds (Figure 5(i), $p > .05$, one-way ANOVA). This NO-mediated decrease in amplitudes was completely abolished by ODQ (Figure 5(j), $p > .05$, one-way ANOVA).

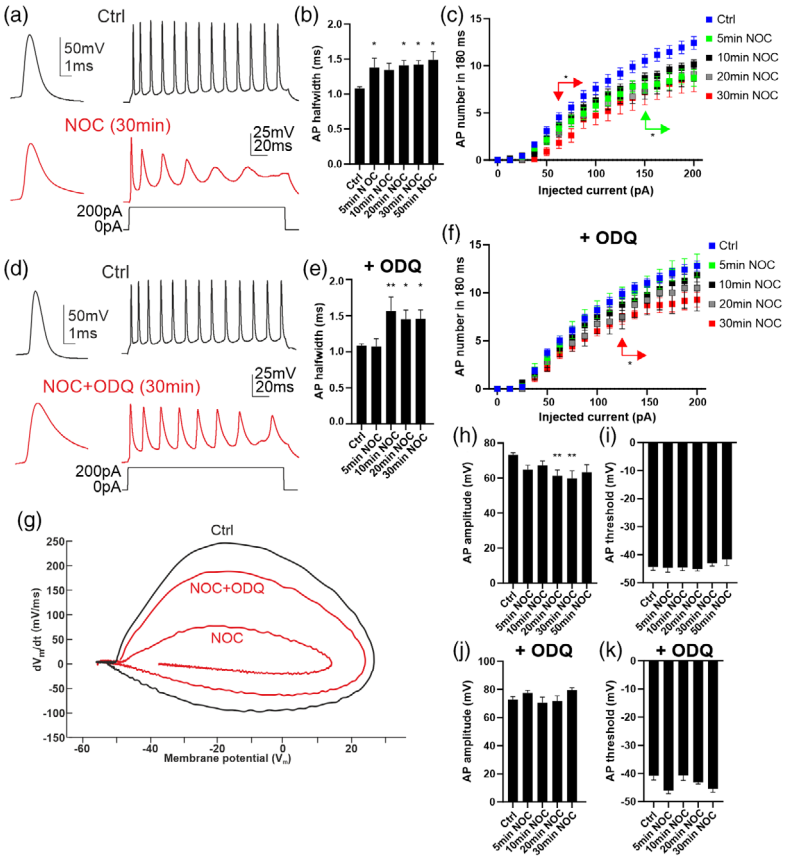

FIGURE 5 Action potential waveform is broadened and depolarization-evoked firing rates are reduced by nitric oxide (NO). (a) Raw traces of single action potentials (APs) and AP firing following a 180 ms 200 pA current injection. (b) Summary data for AP half-width (first AP at rheobase). (c) Effect of NO at different timepoints on AP numbers as a function of injected current. NO causes significant reductions in AP numbers after 5 min above 150 pA current injections (green arrow) and after 30 min exposure already at 62.5 pA and above (red arrow, two-way analysis of variance [ANOVA]). (d) Raw traces of single APs and AP firing following a 180 ms 200 pA current injection. (e) Summary data for AP half-width. (f) Effect of NO at different timepoints on AP numbers as a function of injected current in the presence of ODQ. NO now only causes significant reductions in AP firing after 30 min at and above 125 pA current injections (red arrow, two-way ANOVA). (g) Representative phase plots for the conditions indicted. (h–k) Summary data for AP amplitudes and AP firing thresholds. Data denote mean ± *SEM* ($n = 8–15$ cells). Significance tested by one-way ANOVA with $^{*}p < .05$, $^{**}p < .01$

Together, these data imply two different effects induced by NO. First, an AP widening caused by a reduction in Kv2 currents which was unaffected by ODQ. Second, we noticed a NO-mediated suppression of AP firing rates during the 180 ms depolarization pulse. We further noticed that amplitudes of the initial AP were reduced following NO exposure. Finally, we showed that the maximal dV_m/dt values at the AP rising phase were substantially reduced by NO. These data point toward an additional effect of NO on sodium channel activities. Interestingly, the NO effects on AP amplitudes, firing rates and upstroke values were partially prevented by ODQ (Figure 5(d),f,g,j)).

AP thresholds were unaffected by ODQ treatment (Figure 5(k), $p > .05$, one-way ANOVA). 8-Br-cGMP did not affect any of the AP parameters nor did direct stimulation of the sGC while blocking phosphodiesterase activities (Figure 6; 8-Br-cGMP and YC-1 + IBMX, $p > .05$, one-way ANOVA) with neither condition altering the firing rates during current-evoked depolarization (not shown). Since GSH impacted on Kv current modulation following NO exposure, we next tested whether GSH was also able to recover APs waveforms and firing pattern. Interestingly, GSH completely blocked the effects of NO on AP half-width, again confirming a redox-sensitive component of NO signaling (Figure 7(a,b)). The lack of AP widening also impacted on the excitability, with GSH preventing the decline in firing rates during depolarizing current injections in the presence of NO (Figure 7(c)). When assessing the AP waveform, the phase plots illustrate the actions of GSH on nitrergic changes (Figure 7(d)) with GSH preventing the NO-induced reduction in AP amplitudes (Figure 7(e,f)).

Finally, we wanted to assess how NO affected AP parameters and excitabilities following block of either Kv3 or Kv2 channels by TEA and GxTx-1E, respectively. Blocking Kv3 channels caused a small nonsignificant increase (~10%) in AP half-widths. However, in the presence of TEA, NO caused a further widening of half-widths, whilst activation of the cGMP signaling cascade was without effect (Figure 8(a) [-Kv3], Ctrl vs. TEA + NOC: $p < .0001$, TEA vs. TEA + NOC: $p = .0003$, TEA + YC-1 + IBMX vs. TEA + NOC: $p = .0066$; one-way ANOVA). In contrast, GxTx-1 increased AP half-widths by ~25% as reported previously (Liu & Bean, 2014) with NO having no additional effects (Figure 8(a) [-Kv2], Ctrl vs. GxTx-1: $p = .008$, Ctrl vs. GxTx-1 + NOC: $p = .049$, GxTx-1 vs. GxTx-1 + NOC: $p = .99$, one-way ANOVA). AP amplitudes or firing thresholds were not affected by treatment with either channel blocker (Figure 8(b,c)); however, NO reduced AP amplitudes in the absence of Kv3 (Figure 8(b), TEA vs. TEA + NOC: $p = .0086$, one-way ANOVA). Interestingly, blocking either Kv channel does not reduce AP numbers in responses to short current-induced depolarization as reported previously in the hippocampus following GxTx-1 application (Liu & Bean, 2014). However, additional NO application diminished the number of APs fired in the presence of TEA (at and above 87.5 pA current injection) and GxTx-1 (at and above 75 pA current injection, black arrows, TEA: $p = .0133$, GxTx-1: $p = .0229$, Figure 8(d,e), two-way ANOVA). Together, in agreement with previous reports (Liu & Bean, 2014) our data show

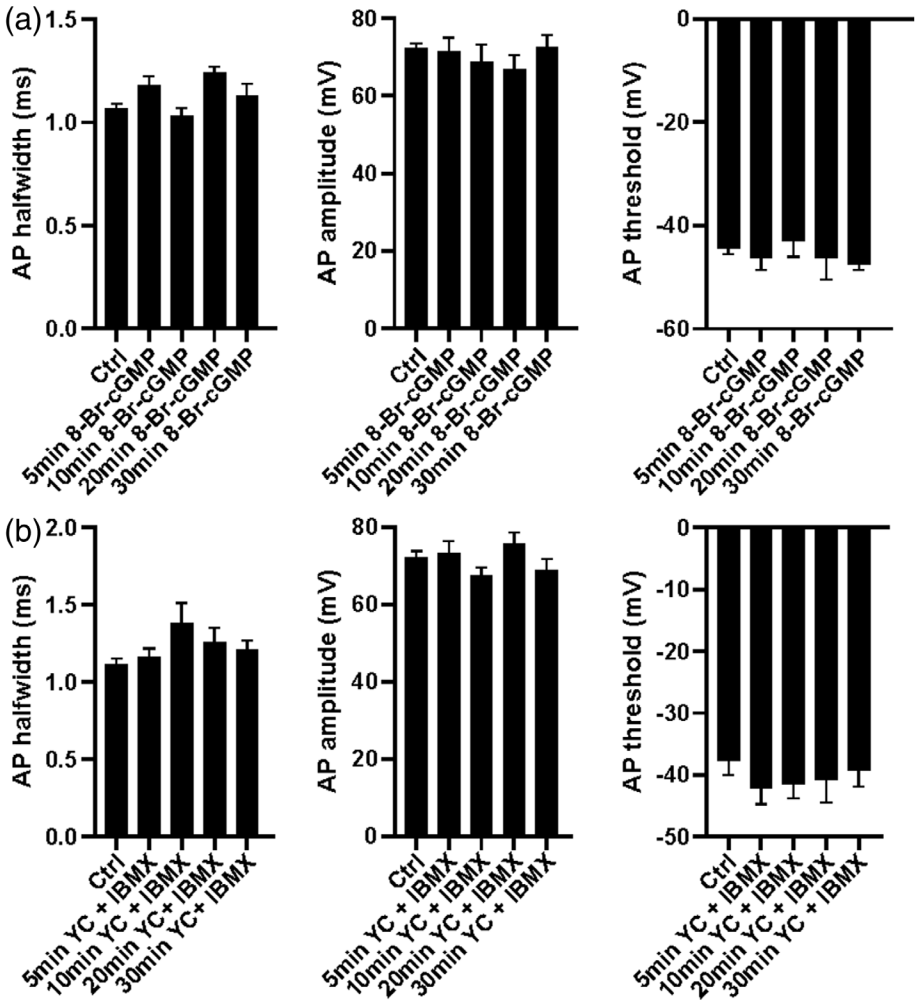

FIGURE 6 Activation of cGMP signaling does not affect action potential waveforms. Summary data of action potential (AP) half-width, amplitude, and threshold following application of 8-Br-cGMP (a) and YC + IBMX (b). Data denote mean ± *SEM* ($n = 6$–18 cells). Significance tested by one-way analysis of variance (ANOVA), $p > .05$

that inhibition of Kv2 in hippocampal neurons had no effect on initial AP firing rates but the observed changes in the current input–output relationships following NO exposure strongly imply that an additional mechanism, for example, reduced sodium channel activity, could be the underlying reason for the reductions in AP numbers.

3.3 | NO suppresses voltage-gated sodium currents in a cGMP-dependent and redox-sensitive manner

The observed decrease in AP amplitudes and a Kv-independent reduction in depolarization-evoked AP firing following NO exposure strongly indicates a modulation of voltage-gated sodium currents (Renganathan et al., 2001). We therefore wanted to test whether voltage-gated sodium channels were directly affected by NO. In baroreceptor neurons and N1E-115 neuroblastoma cells, previous studies have shown that application of NO donors can reduce voltage-gated sodium currents (Ribeiro et al., 2007); however, such data in hippocampal neurons has not yet been reported. At this point, we need to be cautious of voltage and space clamp errors which will impact on measurements of fast and large voltage-gated current recordings in nonspherical neurons (Williams & Mitchell, 2008). However, Na_V current recordings have been reported in CA1 pyramidal neurons in acute brain slices (French et al., 2016; Liu et al., 2017) and applying rigorous criteria to minimize these potential errors, see Methods, enabled us to detect nitrergic effects on current amplitudes. We measured sodium currents activated by a step depolarization from −90 to −30 mV and found that NO reduced current amplitudes following 5–50 min of exposure by about 50% (Figure 9(a–c), one-way ANOVA). To characterize the potential nitrergic signaling routes, we assessed the effects of GSH and ODQ by co-incubating the slices with either drug. In parallel to the observed effects on potassium currents, we found that GSH prevented NO-induced current suppression (Figure 9(d–f)), suggesting that the inhibition of sodium channels might occur via redox signaling. To the contrary to the effects on Kv currents, inhibition of cGMP generation by ODQ also blocked the nitrergic effects (Figure 9(g–l)) indicating that both, cGMP-dependent and -independent nitrergic signaling were required to suppress Na_V currents. This finding also agrees with data obtained on AP amplitudes and upstroke velocities (dV_m/dt) where their reductions by NO were also prevented by both, GSH and ODQ (Figure 5(g–j)). However, when specifically activating the cGMP cascade directly by 8-Br-cGMP or YC-1 + IBMX, both in the absence of NO, we did not observe any effects on sodium currents (Figure 10, $p > .05$,

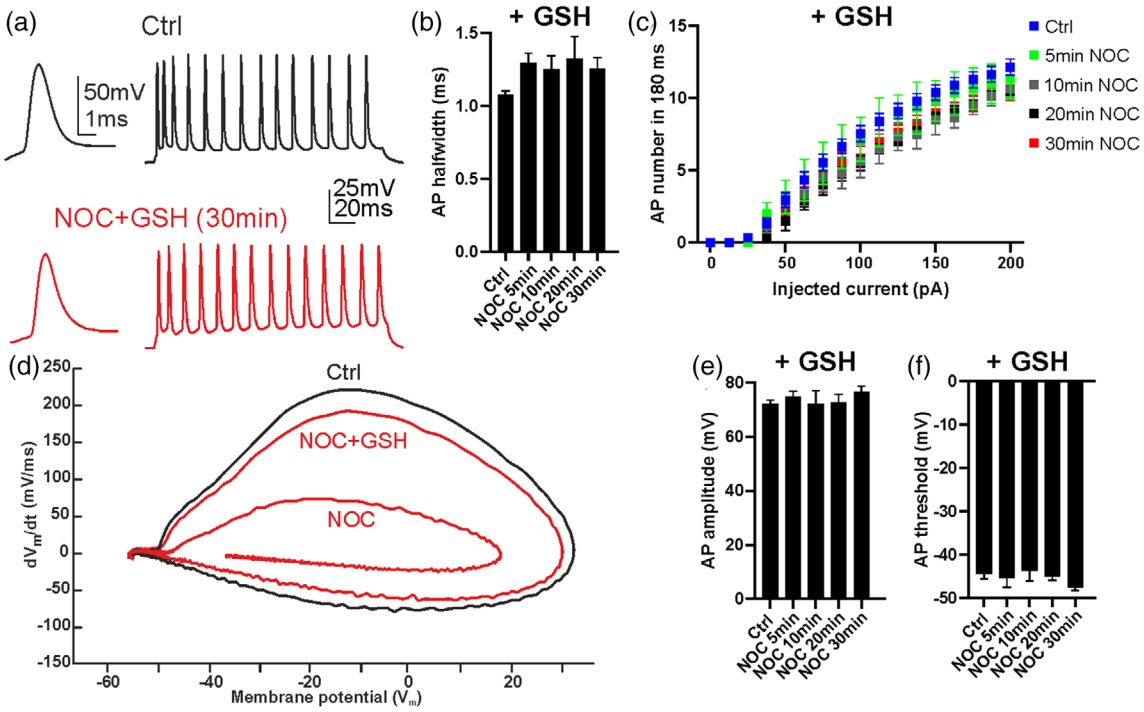

FIGURE 7 Glutathione prevents action potential broadening and diminishes nitrergic effects on depolarization-evoked firing rates. (a) Raw traces of single action potentials (APs) and AP firing following a 180 ms 200 pA current injection. (b) AP half-width of single APs in the presence of glutathione ethyl-ester (GSH). (c) Number of APs following nitric oxide (NO) + GSH incubation at different timepoints as a function of injected current. GSH completely abolishes nitrergic effects on AP numbers at any timepoint (two-way analysis of variance [ANOVA]). (d) Representative phase plots for indicated conditions (NOC trace as in Figure 5(g) for comparison). (e) Summary data for AP amplitudes. (f) Summary data for AP firing thresholds. Data denote mean ± *SEM* ($n = 8$–15 cells). Significance tested by one-way ANOVA, $p > .05$

one-way ANOVA) indicating that cGMP signaling alone is not sufficient to suppress the current.

Accumulating sodium current steady-state inactivation is one of the reasons for reduced AP amplitudes during high-frequency trains (Jung et al., 1997) and may mediate the reduction in firing rates observed in the presence of NO. We thus wanted to test whether NO affected channel inactivation *per se* by applying conditioning pre-depolarizing steps ranging from −90 to −15 mV for 350 ms from a holding potential of −90 mV followed by current activation at −30 mV (modified protocol from Sole et al. (2020)). Boltzmann fit to the relative current amplitudes in control conditions and following NO exposure revealed identical $V_{1/2}$ values, similar to previously reported values for channel inactivation in CA1 pyramidal neurons (Figure 11(a,b), $p > .05$, one-way ANOVA) (French et al., 2016). Furthermore, neither direct activation of the cGMP signaling nor addition of GSH (+NO) revealed any changes in $V_{1/2}$ or slope values (Figure 11(a,b), k_{Ctrl}: −3.1 ± 0.3, k_{NOC}: −4.8 ± 1.8, $k_{NOC + GSH}$: −3.2 ± 0.6, $k_{YC\text{-}1 + IBMX}$: −2.5 ± 0.6, $k_{8\text{-}Br\text{-}cGMP}$: −3.3 ± 0.4, $p > .05$, one-way ANOVA), indicating that the NO-mediated suppression of currents was not due to changes in the inactivation kinetics of the channel. Figure 11(c) summarizes Na_V current data under the investigated conditions (Figure 11(c), averaged data for 10–30 min time points per condition, Ctrl vs. NOC: $p = .0012$, NOC vs. 8-Br-cGMP: $p = .004$, NOC vs. YC-1 + IBMX: $p = .0035$, NOC vs. NOC + ODQ: $p = .0185$, NOC vs. NOC + GSH: $p = .0272$, one-way ANOVA). The data show that GSH or ODQ alone were able to prevent NO effects on sodium current amplitudes which suggests that the channel inhibition requires both pathways to be simultaneously active.

Together, our data illustrate that NO suppresses Kv2 currents in a redox-sensitive manner which translates into wider APs and a reduction in AP firing. However, an additional cGMP- and redox-sensitive component of NO signaling suppresses Na_V currents which reduces AP amplitudes and firing rates independently of, and in addition to, Kv modulation.

4 | DISCUSSION

Our study revealed that NO differentially modulates hippocampal ion channel activities, thereby impacting on neuronal excitabilities and AP waveforms. We provide data illustrating nitrergic suppression of Kv2 channels in intact CA1 pyramidal neurons in a cGMP-independent manner likely due to NO-mediated posttranslational modifications. In addition, we show that NO reduced Na_V currents, however, this NO-mediated effect required simultaneous cGMP-dependent and cGMP-independent redox signaling.

We confirmed that Kv2 current suppression was reversible and prevented by GSH, the most powerful endogenous denitrosylating

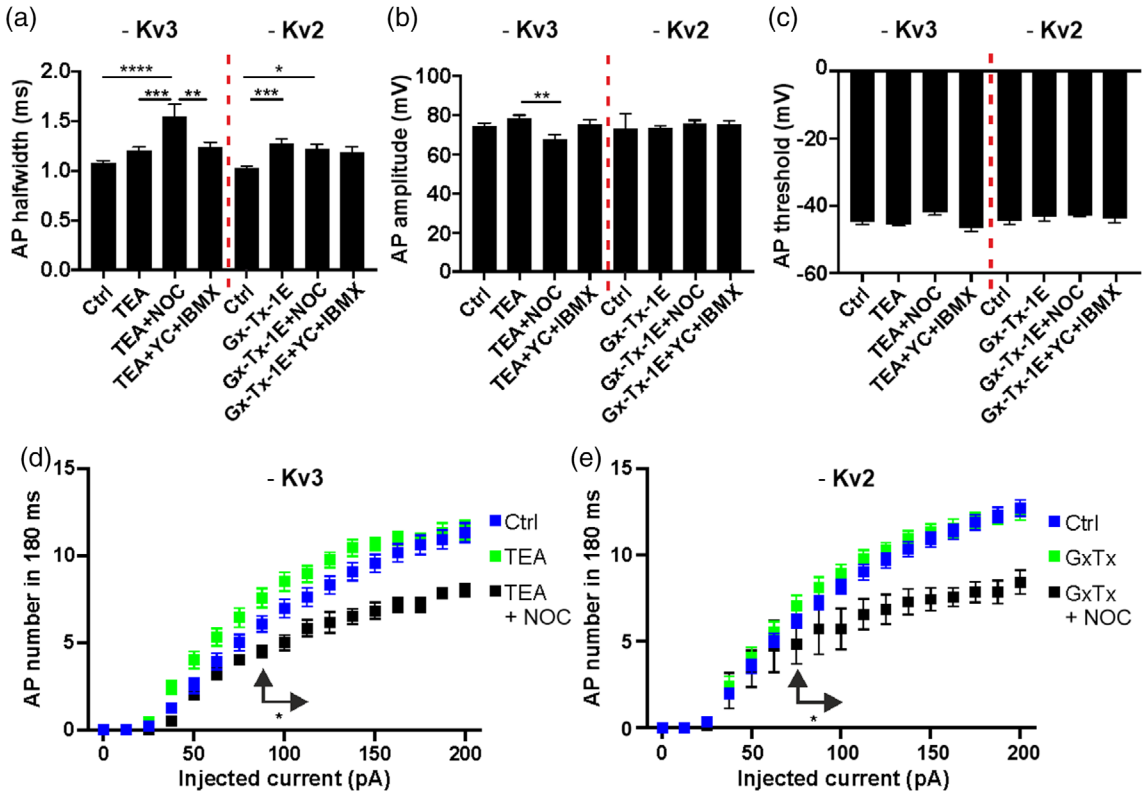

FIGURE 8 Nitric oxide (NO)-induced widening of action potential (AP) half width is abolished by GxTx-1 but not tetraethylammonium (TEA) with neither blocker preventing NO-induced suppression of AP firing rates. (a) Depolarization-evoked AP half-widths. (b) Amplitudes and (c) thresholds for indicated conditions. (d) Number of APs as a function of injected current for 180 ms following incubation with indicted drugs. (e) Number of APs as a function of injected current for 180 ms following incubation with indicted drugs, all drug exposures were between 5 and 10 min. Data denote mean ± *SEM* ($n = 5$–14 cells). Significance tested by one-way analysis of variance (ANOVA) (a–c) and two-way ANOVA (d,e) with $^{*}p < .05$, $^{***}p < .001$, $^{****}p < .0001$

compound (Romero & Bizzozero, 2009; Stomberski et al., 2019), and that activation of the cGMP-PKG cascade by either the non-hydrolysable analogue of cGMP, 8-Br-cGMP (Figure 1(f)) or by the sGC activator YC-1 (Figure 1(e)) did not impact on Kv currents. Sodium currents, on the other hand, were only suppressed by NO when both pathways, redox and cGMP signaling, were active (Figures 9 and 11(c)) and pharmacological suppression of either pathway prevented the nitrergic effects (Figure 11(c)). Furthermore, modulation of both ion channels resulted in a widening of APs and reduction of AP amplitudes. This in turn led to a decrease in depolarization-induced AP firing rates which will have major consequences on information transmission, especially during periods of high activity. The use of our voltage-clamp protocols excluded activation of currents such as mediated by Kv4 and HCN channels. Although not pharmacologically eliminated, our data suggest that suppression of whole-cell outward currents was not involving the Kv7 family, since Kv7 current reduction would reduce AP thresholds, enhance amplitudes, and increase excitability (Carver & Shapiro, 2019)—all of which are opposite effects to the ones observed in our study. Similarly, low voltage-activated Kv1 currents are equally unlikely to be modulated, since we did not detect any changes in currents at voltages negative to 0 mV or AP firing thresholds which are impacted on by this conductance (Coetzee et al., 1999; Jan & Jan, 2012). However, future studies will have to specifically address the question whether Kv7 and Kv1 channels can be modulated by NO in hippocampal CA1 pyramidal neurons which could cause phenotypes of weaker and more modulatory nature.

Hippocampal Kv2.1 channels can undergo PKA-dependent phosphorylation (Ikematsu et al., 2011; Mohapatra et al., 2007), and our data suggest an additional regulatory pathway whereby NO, in a cGMP-independent manner, suppresses Kv2 currents in pyramidal neurons. Interestingly, pharmacological block of Kv2 in CA1 pyramidal neurons only leads to a decrease in AP firing following prolonged depolarizing steps >800 ms (Palacio et al., 2017). In contrast, our data indicate that NO reduces neuronal firing rates after only 100 ms of depolarization (Figure 5(c)) which cannot be attributed to a sole nitrergic effect on Kv2 currents but rather suggests that an additional suppression of sodium currents contributes to the reduction in AP firing rates. As illustrated in the phase plots, NO strongly reduces the maximal upstroke of the AP (dV_m/dt, Figure 5(g)) implicating a suppression of Na_V (Liu & Bean, 2014). Our data show that, only when both, Kv2 and Na_V conductances, are reduced, as would happen following endogenous NO generation, the modulatory action of NO results in complex effects on intrinsic excitability.

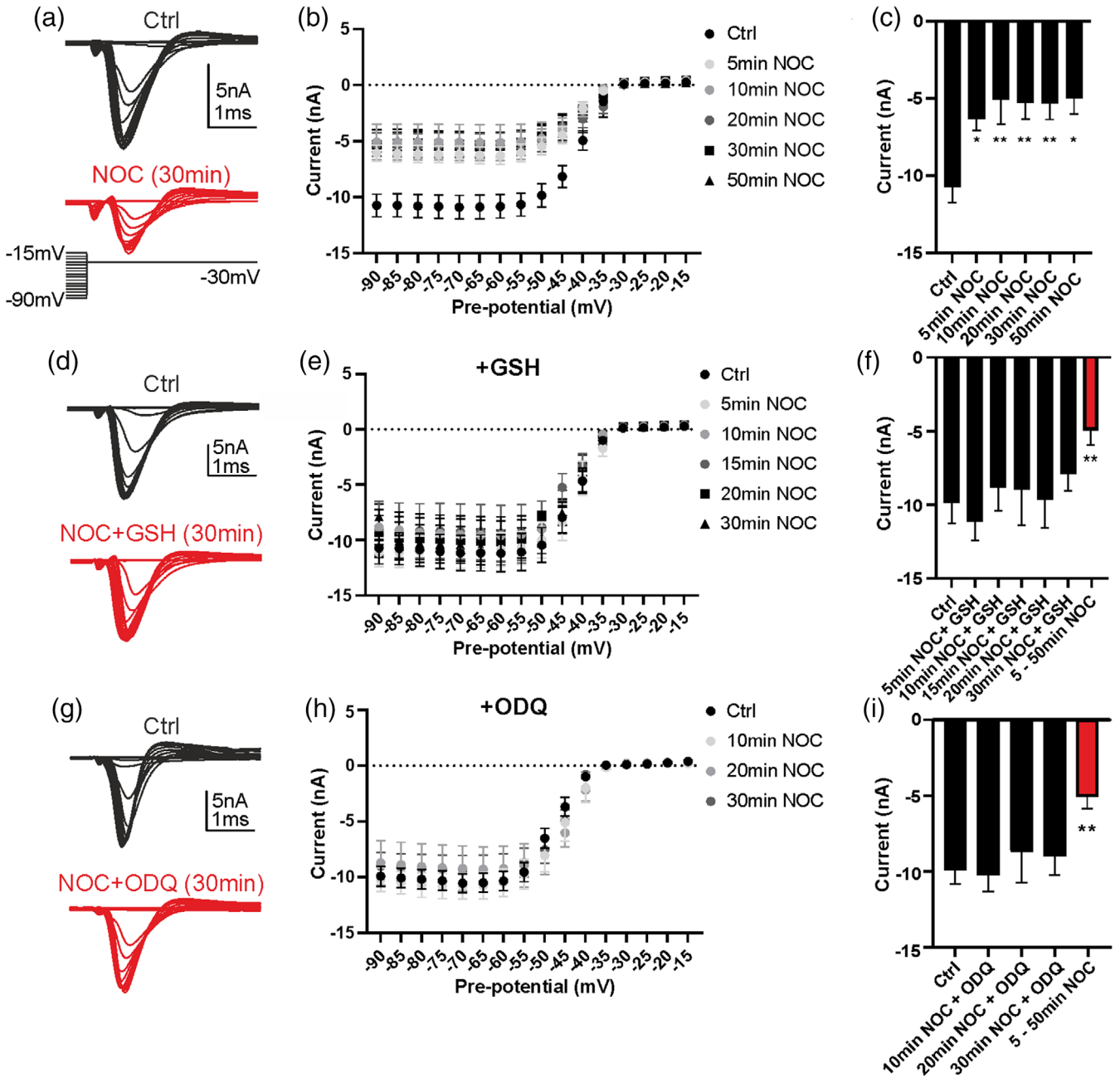

FIGURE 9 Nitric oxide (NO) suppresses voltage-gated sodium currents in a glutathione- and ODQ-dependent manner. (a) Stepwise depolarizations of pyramidal neurons from a holding potential of −90 mV to test potentials between −90 and −15 mV elicited inward sodium currents recorded at −30 mV, see voltage protocol below. (b) Current–voltage relationship for peak current amplitudes at different times of NO incubation. (c) Summary data of peak amplitudes at indicated timepoints measured at maximal depolarization (from −90 to −30 mV). (d) Sample traces of stepwise depolarizations of pyramidal neurons from a holding potential of −90 mV to test potentials between −90 and −15 mV in the presence of NOC + glutathione ethyl-ester (GSH) (d) or NOC + ODQ (g). (e,h) Current–voltage relationship for peak current amplitudes at different times of co-incubation with GSH (e) and ODQ (h). (f,i) Summary data of peak amplitudes at indicated timepoints after co-incubation with NOC + GSH (f) and NOC + QDQ (i). Data denote mean ± *SEM* ($n = 5$–13 cells). Significance tested by one-way analysis of variance (ANOVA) with $^{*}p < .05$, $^{**}p < .01$

NO modulates a wide range of neuronal functions, acting as a crucial signaling molecule in learning and memory and regulation of neuronal plasticity, including processes such as long-term potentiation or fear conditioning. However, overproduction of NO is also associated with neurotoxicity, metabolic dysregulation and neurodegeneration (Bourgognon et al., 2021; Dias et al., 2016; Du et al., 2020; Garthwaite, 2016; Pigott & Garthwaite, 2016; Steinert, Chernova, & Forsythe, 2010). Due to its nature as a volume transmitter, NO acts not only within the neuron of origin but also in neighboring cells, including astrocytes or microvasculature endothelium, a

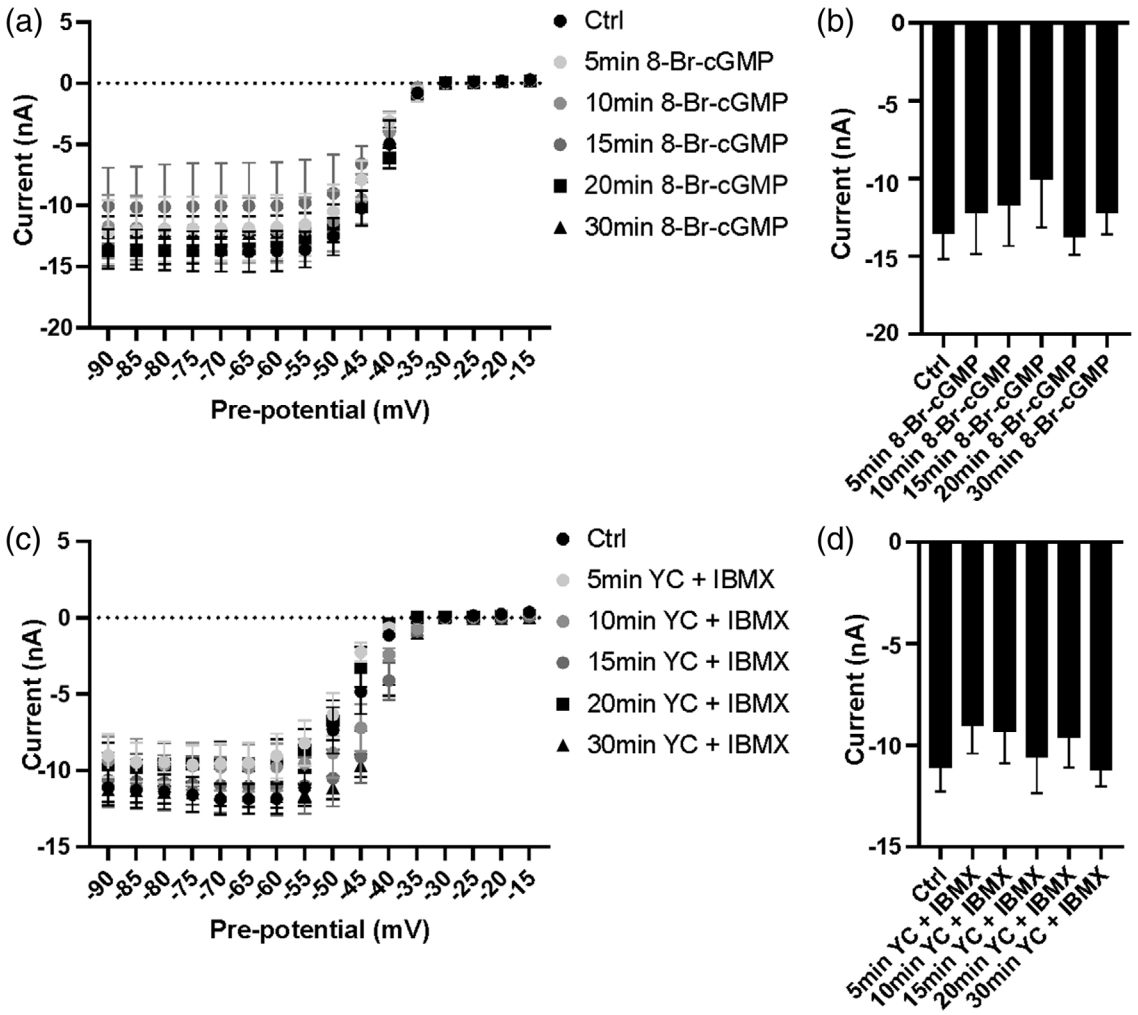

FIGURE 10 Activation of cGMP signaling alone does not affect sodium currents. (a,c) Current–voltage relationship for peak current amplitudes at different times following 8-Br-cGMP (a) and YC + IBMX (c) incubation. (b,d) Summary data of peak amplitudes at indicated timepoints after incubation with 8-Br-cGMP (b) and YC + IBMX (d). Data denote mean ± *SEM* ($n = 5$–13 cells). Significance tested by one-way analysis of variance (ANOVA), $p > .05$

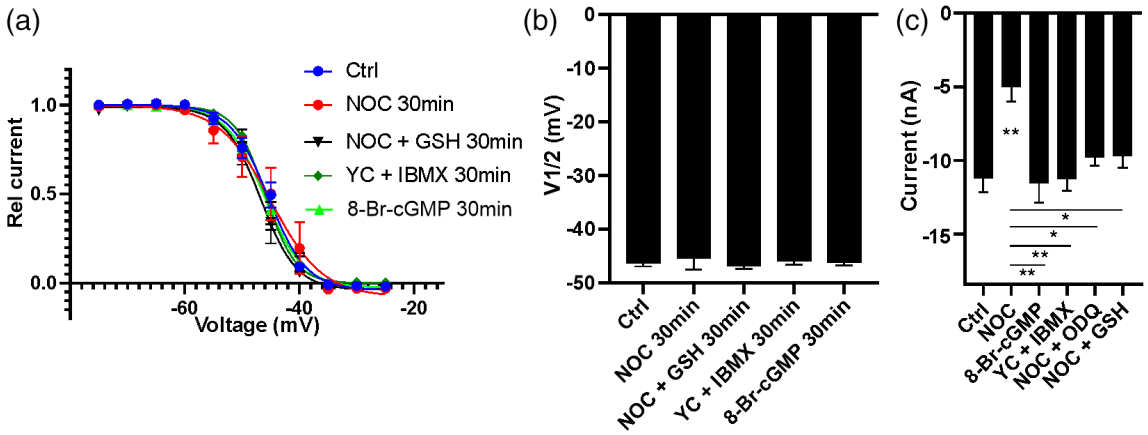

FIGURE 11 Nitrergic effects on sodium currents are not due to changes in channel inactivation. (a) Boltzmann fitting to voltage-dependent inactivation of relative current amplitudes for indicated conditions. (b) Summary of mean $V_{1/2}$ values. (c) Summary of mean current amplitudes, averaged over 10–30 min for each condition. Data denote mean ± *SEM* ($n = 8$–19 cells). Significance tested by one-way analysis of variance (ANOVA) with $^{*}p < .05$, $^{**}p < .01$

mechanism related to neurovascular coupling, where its effects occur in a diffusion-limited space (Artinian et al., 2010; Garthwaite, 2019; Hoiland et al., 2020; Ledo et al., 2015; Lourenco et al., 2017; Philippides et al., 2005).

The multiple actions of NO impacting on the synaptic release machinery and ion channels may be mediated by the canonical cGMP-mediated pathway in addition to specific posttranslational protein modifications (Bradley & Steinert, 2016; Gamper & Ooi, 2015; Robinson et al., 2018). However, the outcome of these processes depends on the rate of production and inactivation of reactive NO molecules and reversal of the downstream signaling, mediated by phosphatases, phosphodiesterases (i.e., PDE-4) or glutathione-mediated de- and trans-nitrosylation events. Consequently, the reported and sometimes controversial actions of NO can be explained by variable exposure times/production rates and uncontrolled activities of above signaling routes or, more importantly, inconsistent concentrations of applied NO (donors), even when assessed within the same cell type. Based on published NO donor release profiles (Bradley & Steinert, 2015), we predicted that the NO concentrations used in our study are in the range of 400–500 nM. Further, we systematically characterized the effects over a time course of 5–50 min and thus our data present a thorough assessment of nitrergic effects on the electrophysiological properties of CA1 pyramidal neurons.

The effects of NO range from Kv3.1 current suppression (donor: 100 μM SNP, 100 μM Papa-NONOate) to increases in Kv2 currents following long-term NO exposure (>80 min) in principal neurons in the MNTB and pyramidal hippocampal CA3 neurons which involves phosphorylation-dependent pathways (Steinert et al., 2008; Steinert et al., 2011). Various reported physiological differences in responses to NO release (exposure) between brain regions illustrate the heterogeneity of this signaling. For example, the density of nNOS expressing principal neurons in the MNTB is higher compared to densities in the hippocampus and even within the hippocampus, CA1 and CA3 regions show different densities of nNOS positive neurons (Jinno & Kosaka, 2002; Steinert et al., 2008). Thus, a neuron's NO exposure and response can differ drastically between brain regions and, even more confoundingly, developmental stages. In the hippocampus, there is a transient expression of nNOS in the pyramidal cell layer at P3–P7, which by P14 shows a reduced expression. At P21, there is a general lower expression which is comparable to adulthood (Chung et al., 2004) suggesting that endogenous NMDAR-dependent NO productions declines with age. We have previously shown in mouse, that the size of NMDAR-mediated currents declined with age reaching relatively comparable amplitudes between P14 and P21 (in the auditory brainstem (Steinert, Postlethwaite, et al., 2010)) suggesting again an age-dependent decline in NMADR-mediated NO generation.

The volume diffusion of NO can occur with a radius of several tens of micrometers (Lourenco, Santos, et al., 2014; Philippides et al., 2005) and at concentrations as low as fmolar to pmolar whilst lasting several seconds at these levels (Batchelor et al., 2010; Lourenco, Ferreira, et al., 2014), indicating that volume transmitting has the ability to induce signaling within larger brain regions when released by a single neuron. The release profile of endogenously produced NO in response to NMDA perfusion into rat CA1 hippocampal regions shows a transient increase in NO levels between 100 and 350 nM (10–100 μM NMDA) (Ledo et al., 2005; Ledo et al., 2010). Importantly, different NO release profiles between the hippocampal CA1/CA3/dentate gyrus regions have been detected following transient glutamate injection into hippocampal brain slices from 8 to 10 weeks old rats (Lourenco, Ferreira, et al., 2014). The amounts of released NO vary drastically between the regions with peak levels reaching 3–4 fmol s^{-1}, lasting several tens of seconds. Other reports show NO levels of several tens up to 300 pmol released in the cerebellum or hippocampus of P8–P10 old rats (Wood et al., 2011)—again, note that a younger age correlates with increased NO release. Due to the improvements of recording methods over the years, it is now possible to detect physiologically relevant NO concentrations although due to different methodologies (optical vs. electrochemical) and differences in animal ages, data comparisons are still difficult.

Due to the differences in NOS expression and NO generation between neurons and brain regions, reported physiological in vivo effects of NO signaling also vary greatly. In the auditory system, in vivo NO generation suppresses sound-evoked firing without affected basal activities (Hockley et al., 2020). Conversely, inhibition of NOS prevents the nicotine-induced increase in firing activity in neurons of the substantia nigra pars compacta without affecting their basal activities (Di Matteo et al., 2010). As these data reflect extracellular field recordings, it is difficult to conclude how NO acts on the level of ion channels. The vast amount of available and seemingly inconsistent data on NO signaling, further complicated by discrepancies between in vivo and in vitro conditions, makes this signaling route to one of the most studied, yet large gaps in our understanding remain. Our data offer new insights how NO can modulate intrinsic excitabilities in the hippocampus which potentially links activity-dependent NO generation to changes in activities of ion channels, such as Na_V and Kv2, responsible for membrane depolarization and hyperpolarization, respectively.

Our findings might be able to explain discrepancies between data obtained under in vivo and in vitro conditions. It has been long established that neuronal properties differ between the artificial slice preparations and in vivo environments. A recent study of a direct comparison of pyramidal neurons of the Layer 2/3 somatosensory cortex revelated that APs are broader and current-evoked firing frequencies are lower in vivo compared to in vitro (Fernandez et al., 2018). Although the authors only presented this observation and did not suggest any mechanisms, a likely relation to our findings could be an activity-dependent in vivo modulation of Kv2 and Na_V currents by NO resulting in the observed differences.

The findings reported in our study may also have implications for regulating neuronal excitability following acute changes in hippocampal firing patterns and activity-driven NO generation, such as occur during traumatic brain injuries, epileptiform or changes in temporal spiking properties during fundamental computational activities (Ding et al., 2020; Ghotbeddin et al., 2019; Karimi et al., 2020; Martin et al., 2019; Song et al., 2020).

The use of NO donors provides an essential tool to study nitrergic effects, although unphysiologically high NO levels being released by various donors, pathological and disease-relevant iNOS-mediated NO release will be substantially higher and thus compare to higher NO donor release profiles. Numerous ion channel targets for NO signaling have been reported in in vitro preparations which provides detailed information on NO's ability to regulate neuronal excitability. In *Helisoma trivolvis* snail B19 neurons, NO (100 μM NOC-7, 100 μM DEA-NONOate) inhibits SK (small calcium-activated potassium channel) as well as voltage-gated potassium channels but endogenous NO production enhances calcium and persistent sodium currents thereby adjusting neuronal excitability (Artinian et al., 2010; Artinian et al., 2012; Estes et al., 2015; Zhong et al., 2013, 2015). NO inhibits voltage-gated and persistent sodium currents in C-type DRG neurons over a time course of up to 40 min via S-nitrosylation (Papa-NONOate [IC_{50}: 750 μM] (Renganathan et al., 2002)) and modulates TRPV1 (Han et al., 2017), cyclic nucleotide-gated ion channels in magnocellular neurosecretory cells (Pires da Silva et al., 2016), K_{ATP} channels in DRG neurons (Kawano et al., 2009) and Kv7.1/Kv7.4 in the trigeminal ganglia (Asada et al., 2009; Ooi et al., 2013) via S-nitrosylation with different outcomes for intrinsic excitabilities and our findings extend information on nitrergic action in the hippocampus.

Future studies will have to identify whether the modulation of Na_V channels by NO occurs directly on the channel protein or indirectly via other forms of posttranslational modifications such as phosphorylation or S-nitrosylation. Although it will have to be elucidated which exact posttranslational protein modifications occur on both ion channels, our data support the notion that activity-driven NO production might act as a feedback regulator to adjust ion channel activities and thus firing rates within in vivo networks.

ACKNOWLEDGMENTS

The authors thank Prof Giovanni Mann (King's College London, UK) and Dr Jereme Spiers (La Trobe University, Australia) for their helpful discussions in preparation of this manuscript. This work was supported by the Medical Research Council (MC_U132681855), UK.

CONFLICT OF INTEREST

The authors declare no conflict of interest.

AUTHOR CONTRIBUTIONS

Joern R. Steinert and **Hannah Scheiblich**: Designed research. **Hannah Scheiblich**: Performed experiments. **Joern R. Steinert** and **Hannah Scheiblich**: Analyzed the data and wrote the paper.

DATA AVAILABILITY STATEMENT

The data that support the findings of this study are available from the corresponding author upon reasonable request.

ORCID

Joern R. Steinert https://orcid.org/0000-0003-1640-0845

REFERENCES

Akhtar, M. W., Sunico, C. R., Nakamura, T., & Lipton, S. A. (2012). Redox regulation of protein function via cysteine S-nitrosylation and its relevance to neurodegenerative diseases. *International Journal of Cell Biology*, *2012*, 463756. https://doi.org/10.1155/2012/463756

Artinian, L., Tornieri, K., Zhong, L., Baro, D., & Rehder, V. (2010). Nitric oxide acts as a volume transmitter to modulate electrical properties of spontaneously firing neurons via apamin-sensitive potassium channels. *The Journal of Neuroscience*, *30*(5), 1699–1711. https://doi.org/10.1523/JNEUROSCI.4511-09.2010

Artinian, L., Zhong, L., Yang, H., & Rehder, V. (2012). Nitric oxide as intracellular modulator: Internal production of NO increases neuronal excitability via modulation of several ionic conductances. *The European Journal of Neuroscience*, *36*(10), 3333–3343. https://doi.org/10.1111/j.1460-9568.2012.08260.x

Asada, K., Kurokawa, J., & Furukawa, T. (2009). Redox- and calmodulin-dependent S-nitrosylation of the KCNQ1 channel. *The Journal of Biological Chemistry*, *284*(9), 6014–6020. https://doi.org/10.1074/jbc.M807158200

Bae, H., Kim, T., & Lim, I. (2020). Effects of nitric oxide on apoptosis and voltage-gated calcium channels in human cardiac myofibroblasts. *Clinical and Experimental Pharmacology & Physiology*, *47*(1), 16–26. https://doi.org/10.1111/1440-1681.13178

Balez, R., & Ooi, L. (2016). Getting to NO Alzheimer's disease: Neuroprotection versus neurotoxicity mediated by nitric oxide. *Oxidative Medicine and Cellular Longevity*, *2016*, 3806157. https://doi.org/10.1155/2016/3806157

Batchelor, A. M., Bartus, K., Reynell, C., Constantinou, S., Halvey, E. J., Held, K. F., Dostmann, W. R., Vernon, J., & Garthwaite, J. (2010). Exquisite sensitivity to subsecond, picomolar nitric oxide transients conferred on cells by guanylyl cyclase-coupled receptors. *Proceedings of the National Academy of Sciences of the United States of America*, *107*(51), 22060–22065. https://doi.org/10.1073/pnas.1013147107

Bean, B. P. (2007). The action potential in mammalian central neurons. *Nature Reviews. Neuroscience*, *8*(6), 451–465. https://doi.org/10.1038/nrn2148

Bourgognon, J. M., Spiers, J. G., Robinson, S. W., Scheiblich, H., Glynn, P., Ortori, C., Bradley, S. J., Tobin, A. B., & Steinert, J. R. (2021). Inhibition of neuroinflammatory nitric oxide signaling suppresses glycation and prevents neuronal dysfunction in mouse prion disease. *Proceedings of the National Academy of Sciences of the United States of America*, *118*(10), e2009579118. https://doi.org/10.1073/pnas.2009579118

Bradley, S. A., & Steinert, J. R. (2015). Characterisation and comparison of temporal release profiles of nitric oxide generating donors. *Journal of Neuroscience Methods*, *245*, 116–124. https://doi.org/10.1016/j.jneumeth.2015.02.024

Bradley, S. A., & Steinert, J. R. (2016). Nitric oxide-mediated posttranslational modifications: Impacts at the synapse. *Oxidative Medicine and Cellular Longevity*, *2016*, 5681036. https://doi.org/10.1155/2016/5681036

Bradley, S. J., Bourgognon, J. M., Sanger, H. E., Verity, N., Mogg, A. J., White, D. J., … Tobin, A. B. (2017). M1 muscarinic allosteric modulators slow prion neurodegeneration and restore memory loss. *The Journal of Clinical Investigation*, *127*(2), 487–499. https://doi.org/10.1172/JCI87526

Brickley, S. G., Revilla, V., Cull-Candy, S. G., Wisden, W., & Farrant, M. (2001). Adaptive regulation of neuronal excitability by a voltage-independent potassium conductance. *Nature*, *409*(6816), 88–92. https://doi.org/10.1038/35051086

Carver, C. M., & Shapiro, M. S. (2019). Gq-coupled muscarinic receptor enhancement of KCNQ2/3 channels and activation of TRPC channels in multimodal control of excitability in dentate gyrus granule cells. *The Journal of Neuroscience*, *39*(9), 1566–1587. https://doi.org/10.1523/JNEUROSCI.1781-18.2018

Choudhury, N., Linley, D., Richardson, A., Anderson, M., Robinson, S. W., Marra, V., Ciampani, V., Walter, S. M., Kopp-Scheinpflug, C., Steinert, J. R., & Forsythe, I. D. (2020). Kv3.1 and Kv3.3 subunits differentially contribute to Kv3 channels and action potential repolarization in principal neurons of the auditory brainstem. *The Journal of Physiology*, *598*(11), 2199–2222. https://doi.org/10.1113/JP279668

Chung, Y. H., Kim, Y. S., & Lee, W. B. (2004). Distribution of neuronal nitric oxide synthase-immunoreactive neurons in the cerebral cortex and hippocampus during postnatal development. *Journal of Molecular Histology*, *35*(8–9), 765–770. https://doi.org/10.1007/s10735-004-0667-2

Clementi, E., Brown, G. C., Feelisch, M., & Moncada, S. (1998). Persistent inhibition of cell respiration by nitric oxide: Crucial role of S-nitrosylation of mitochondrial complex I and protective action of glutathione. *Proceedings of the National Academy of Sciences of the United States of America*, *95*(13), 7631–7636. https://doi.org/10.1073/pnas.95.13.7631

Coetzee, W. A., Amarillo, Y., Chiu, J., Chow, A., Lau, D., McCormack, T., … Rudy, B. (1999). Molecular diversity of K+ channels. *Annals of the New York Academy of Sciences*, *868*, 233–285. https://doi.org/10.1111/j.1749-6632.1999.tb11293.x

Cummins, T. R., Rush, A. M., Estacion, M., Dib-Hajj, S. D., & Waxman, S. G. (2009). Voltage-clamp and current-clamp recordings from mammalian DRG neurons. *Nature Protocols*, *4*(8), 1103–1112. https://doi.org/10.1038/nprot.2009.91

di Matteo, V., Pierucci, M., Benigno, A., Esposito, E., Crescimanno, G., & di Giovanni, G. (2010). Critical role of nitric oxide on nicotine-induced hyperactivation of dopaminergic nigrostriatal system: Electrophysiological and neurochemical evidence in rats. *CNS Neuroscience & Therapeutics*, *16*(3), 127–136. https://doi.org/10.1111/j.1755-5949.2010.00136.x

Dias, C., Lourenco, C. F., Ferreiro, E., Barbosa, R. M., Laranjinha, J., & Ledo, A. (2016). Age-dependent changes in the glutamate-nitric oxide pathway in the hippocampus of the triple transgenic model of Alzheimer's disease: Implications for neurometabolic regulation. *Neurobiology of Aging*, *46*, 84–95. https://doi.org/10.1016/j.neurobiolaging.2016.06.012

Ding, L., Chen, H., Diamantaki, M., Coletta, S., Preston-Ferrer, P., & Burgalossi, A. (2020). Structural correlates of CA2 and CA3 pyramidal cell activity in freely-moving mice. *The Journal of Neuroscience*, *40*(30), 5797–5806. https://doi.org/10.1523/JNEUROSCI.0099-20.2020

Du, C. P., Wang, M., Geng, C., Hu, B., Meng, L., Xu, Y., … Hou, X. Y. (2020). Activity-induced SUMOylation of neuronal nitric oxide synthase is associated with plasticity of synaptic transmission and extracellular signal-regulated kinase 1/2 signaling. *Antioxidants & Redox Signaling*, *32*(1), 18–34. https://doi.org/10.1089/ars.2018.7669

Du, J., Haak, L. L., Phillips-Tansey, E., Russell, J. T., & McBain, C. J. (2000). Frequency-dependent regulation of rat hippocampal somato-dendritic excitability by the K+ channel subunit Kv2.1. *Journal of Physiology*, *522*(Pt 1), 19–31. https://doi.org/10.1111/j.1469-7793.2000.t01-2-00019.xm

Du, J., Zhang, L., Weiser, M., Rudy, B., & McBain, C. J. (1996). Developmental expression and functional characterization of the potassium-channel subunit Kv3.1b in parvalbumin-containing interneurons of the rat hippocampus. *The Journal of Neuroscience*, *16*(2), 506–518.

Estes, S., Zhong, L. R., Artinian, L., Tornieri, K., & Rehder, V. (2015). The role of action potentials in determining neuron-type-specific responses to nitric oxide. *Developmental Neurobiology*, *75*(5), 435–451. https://doi.org/10.1002/dneu.22233

Fernandez, F. R., Rahsepar, B., & White, J. A. (2018). Differences in the electrophysiological properties of mouse somatosensory layer 2/3 neurons in vivo and slice stem from intrinsic sources rather than a network-generated high conductance state. *eNeuro*, *5*(2), ENEURO.0447–ENEU17.2018. https://doi.org/10.1523/ENEURO.0447-17.2018

French, C. R., Zeng, Z., Williams, D. A., Hill-Yardin, E. L., & O'Brien, T. J. (2016). Properties of an intermediate-duration inactivation process of the voltage-gated sodium conductance in rat hippocampal CA1 neurons. *Journal of Neurophysiology*, *115*(2), 790–802. https://doi.org/10.1152/jn.01000.2014

Friebe, A., Mullershausen, F., Smolenski, A., Walter, U., Schultz, G., & Koesling, D. (1998). YC-1 potentiates nitric oxide- and carbon monoxide-induced cyclic GMP effects in human platelets. *Molecular Pharmacology*, *54*(6), 962–967. https://doi.org/10.1124/mol.54.6.962

Gamper, N., & Ooi, L. (2015). Redox and nitric oxide-mediated regulation of sensory neuron ion channel function. *Antioxidants & Redox Signaling*, *22*(6), 486–504. https://doi.org/10.1089/ars.2014.5884

Garthwaite, J. (2016). From synaptically localized to volume transmission by nitric oxide. *The Journal of Physiology*, *594*(1), 9–18. https://doi.org/10.1113/JP270297

Garthwaite, J. (2019). NO as a multimodal transmitter in the brain: Discovery and current status. *British Journal of Pharmacology*, *176*(2), 197–211. https://doi.org/10.1111/bph.14532

Garthwaite, J., Southam, E., Boulton, C. L., Nielsen, E. B., Schmidt, K., & Mayer, B. (1995). Potent and selective inhibition of nitric oxide-sensitive guanylyl cyclase by 1H-[1,2,4]oxadiazolo[4,3-a]quinoxalin-1-one. *Molecular Pharmacology*, *48*(2), 184–188.

Ghotbeddin, Z., Heysieattalab, S., Borjkhani, M., Mirnajafi-Zadeh, J., Semnanian, S., Hosseinmardi, N., & Janahmadi, M. (2019). Ca(2+) channels involvement in low-frequency stimulation-mediated suppression of intrinsic excitability of hippocampal CA1 pyramidal cells in a rat amygdala kindling model. *Neuroscience*, *406*, 234–248. https://doi.org/10.1016/j.neuroscience.2019.03.012

Han, T., Tang, Y., Li, J., Xue, B., Gong, L., Li, J., Yu, X., & Liu, C. (2017). Nitric oxide donor protects against acetic acid-induced gastric ulcer in rats via S-nitrosylation of TRPV1 on vagus nerve. *Scientific Reports*, *7*(1), 2063. https://doi.org/10.1038/s41598-017-02275-1

Hockley, A., Berger, J. I., Smith, P. A., Palmer, A. R., & Wallace, M. N. (2020). Nitric oxide regulates the firing rate of neuronal subtypes in the Guinea pig ventral cochlear nucleus. *The European Journal of Neuroscience*, *51*(4), 963–983. https://doi.org/10.1111/ejn.14572

Hoiland, R. L., Caldwell, H. G., Howe, C. A., Nowak-Fluck, D., Stacey, B. S., Bailey, D. M., … Ainslie, P. N. (2020). Nitric oxide is fundamental to neurovascular coupling in humans. *The Journal of Physiology*, *598*, 4927–4939. https://doi.org/10.1113/JP280162

Ikematsu, N., Dallas, M. L., Ross, F. A., Lewis, R. W., Rafferty, J. N., David, J. A., Suman, R., Peers, C., Hardie, D. G., & Evans, A. M. (2011). Phosphorylation of the voltage-gated potassium channel Kv2.1 by AMP-activated protein kinase regulates membrane excitability. *Proceedings of the National Academy of Sciences of the United States of America*, *108*(44), 18132–18137. https://doi.org/10.1073/pnas.1106201108

Jan, L. Y., & Jan, Y. N. (2012). Voltage-gated potassium channels and the diversity of electrical signalling. *The Journal of Physiology*, *590*(11), 2591–2599. https://doi.org/10.1113/jphysiol.2011.224212

Jinno, S., Aika, Y., Fukuda, T., & Kosaka, T. (1999). Quantitative analysis of neuronal nitric oxide synthase-immunoreactive neurons in the mouse hippocampus with optical disector. *The Journal of Comparative Neurology*, *410*(3), 398–412.

Jinno, S., & Kosaka, T. (2002). Patterns of expression of calcium binding proteins and neuronal nitric oxide synthase in different populations of hippocampal GABAergic neurons in mice. *The Journal of Comparative Neurology*, *449*(1), 1–25. https://doi.org/10.1002/cne.10251

Jung, H. Y., Mickus, T., & Spruston, N. (1997). Prolonged sodium channel inactivation contributes to dendritic action potential attenuation in hippocampal pyramidal neurons. *The Journal of Neuroscience*, *17*(17), 6639–6646.

Karimi, S. A., Hosseinmardi, N., Sayyah, M., Hajisoltani, R., & Janahmadi, M. (2020). Enhancement of intrinsic neuronal excitability-mediated by a reduction in hyperpolarization-activated cation current

(lh) in hippocampal CA1 neurons in a rat model of traumatic brain injury. *Hippocampus*, *31*, 156–169. https://doi.org/10.1002/hipo.23270

Kawano, T., Zoga, V., Kimura, M., Liang, M. Y., Wu, H. E., Gemes, G., McCallum, J. B., Kwok, W. M., Hogan, Q. H., & Sarantopoulos, C. D. (2009). Nitric oxide activates ATP-sensitive potassium channels in mammalian sensory neurons: Action by direct S-nitrosylation. *Molecular Pain*, *5*, 12. https://doi.org/10.1186/1744-8069-5-12

Kirizs, T., Kerti-Szigeti, K., Lorincz, A., & Nusser, Z. (2014). Distinct axo-somato-dendritic distributions of three potassium channels in CA1 hippocampal pyramidal cells. *The European Journal of Neuroscience*, *39* (11), 1771–1783. https://doi.org/10.1111/ejn.12526

Ledo, A., Barbosa, R., Cadenas, E., & Laranjinha, J. (2010). Dynamic and interacting profiles of *NO and O2 in rat hippocampal slices. *Free Radical Biology & Medicine*, *48*(8), 1044–1050. https://doi.org/10.1016/j.freeradbiomed.2010.01.024

Ledo, A., Barbosa, R. M., Gerhardt, G. A., Cadenas, E., & Laranjinha, J. (2005). Concentration dynamics of nitric oxide in rat hippocampal subregions evoked by stimulation of the NMDA glutamate receptor. *Proceedings of the National Academy of Sciences of the United States of America*, *102*(48), 17483–17488. https://doi.org/10.1073/pnas.0503624102

Ledo, A., Lourenco, C. F., Caetano, M., Barbosa, R. M., & Laranjinha, J. (2015). Age-associated changes of nitric oxide concentration dynamics in the central nervous system of Fisher 344 rats. *Cellular and Molecular Neurobiology*, *35*(1), 33–44. https://doi.org/10.1007/s10571-014-0115-0

Lee, S., Milescu, M., Jung, H. H., Lee, J. Y., Bae, C. H., Lee, C. W., Kim, H. H., Swartz, K. J., & Kim, J. I. (2010). Solution structure of GxTX-1E, a high-affinity tarantula toxin interacting with voltage sensors in Kv2.1 potassium channels. *Biochemistry*, *49*(25), 5134–5142. https://doi.org/10.1021/bi100246u

Lien, C. C., Martina, M., Schultz, J. H., Ehmke, H., & Jonas, P. (2002). Gating, modulation and subunit composition of voltage-gated K(+) channels in dendritic inhibitory interneurones of rat hippocampus. *The Journal of Physiology*, *538*(Pt 2), 405–419. https://doi.org/10.1113/jphysiol.2001.013066

Lipton, S. A., Singel, D. J., & Stamler, J. S. (1994). Neuroprotective and neurodestructive effects of nitric oxide and redox congeners. *Annals of the New York Academy of Sciences*, *738*, 382–387. https://doi.org/10.1111/j.1749-6632.1994.tb21826.x

Liu, P. W., & Bean, B. P. (2014). Kv2 channel regulation of action potential repolarization and firing patterns in superior cervical ganglion neurons and hippocampal CA1 pyramidal neurons. *The Journal of Neuroscience*, *34*(14), 4991–5002. https://doi.org/10.1523/JNEUROSCI.1925-13.2014

Liu, Z.-B., Liu, C., Zeng, B., Huang, L.-P., & Yao, L.-H. (2017). Modulation effects of cordycepin on voltage-gated sodium channels in rat hippocampal CA1 pyramidal neurons in the presence/absence of oxygen. *Neural Plasticity*, *2017*, 2459053. https://doi.org/10.1155/2017/2459053

Lourenco, C. F., Ferreira, N. R., Santos, R. M., Lukacova, N., Barbosa, R. M., & Laranjinha, J. (2014). The pattern of glutamate-induced nitric oxide dynamics in vivo and its correlation with nNOS expression in rat hippocampus, cerebral cortex and striatum. *Brain Research*, *1554*, 1–11. https://doi.org/10.1016/j.brainres.2014.01.030

Lourenco, C. F., Ledo, A., Barbosa, R. M., & Laranjinha, J. (2017). Neurovascular-neuroenergetic coupling axis in the brain: Master regulation by nitric oxide and consequences in aging and neurodegeneration. *Free Radical Biology & Medicine*, *108*, 668–682. https://doi.org/10.1016/j.freeradbiomed.2017.04.026

Lourenco, C. F., Santos, R. M., Barbosa, R. M., Cadenas, E., Radi, R., & Laranjinha, J. (2014). Neurovascular coupling in hippocampus is mediated via diffusion by neuronal-derived nitric oxide. *Free Radical Biology & Medicine*, *73*, 421–429. https://doi.org/10.1016/j.freeradbiomed.2014.05.021

Lu, Y. F., & Hawkins, R. D. (2002). Ryanodine receptors contribute to cGMP-induced late-phase LTP and CREB phosphorylation in the hippocampus. *Journal of Neurophysiology*, *88*(3), 1270–1278. https://doi.org/10.1152/jn.2002.88.3.1270

Martin, S. J., Shires, K. L., & da Silva, B. M. (2019). Hippocampal lateralization and synaptic plasticity in the intact rat: No left-right asymmetry in electrically induced CA3-CA1 long-term potentiation. *Neuroscience*, *397*, 147–158. https://doi.org/10.1016/j.neuroscience.2018.11.044

Martina, M., Schultz, J. H., Ehmke, H., Monyer, H., & Jonas, P. (1998). Functional and molecular differences between voltage-gated K+ channels of fast-spiking interneurons and pyramidal neurons of rat hippocampus. *The Journal of Neuroscience*, *18*(20), 8111–8125.

Megias, M., Verduga, R., Fernandez-Viadero, C., & Crespo, D. (1997). Neurons co-localizing calretinin immunoreactivity and reduced nicotinamide adenine dinucleotide phosphate diaphorase (NADPH-d) activity in the hippocampus and dentate gyrus of the rat. *Brain Research*, *744* (1), 112–120. https://doi.org/10.1016/s0006-8993(96)01075-x

Misonou, H., Mohapatra, D. P., Park, E. W., Leung, V., Zhen, D., Misonou, K., Anderson, A. E., & Trimmer, J. S. (2004). Regulation of ion channel localization and phosphorylation by neuronal activity. *Nature Neuroscience*, *7*(7), 711–718. https://doi.org/10.1038/nn1260

Mohapatra, D. P., Misonou, H., Pan, S. J., Held, J. E., Surmeier, D. J., & Trimmer, J. S. (2009). Regulation of intrinsic excitability in hippocampal neurons by activity-dependent modulation of the KV2.1 potassium channel. *Channels (Austin, Tex.)*, *3*(1), 46–56. https://doi.org/10.4161/chan.3.1.7655

Mohapatra, D. P., Park, K. S., & Trimmer, J. S. (2007). Dynamic regulation of the voltage-gated Kv2.1 potassium channel by multisite phosphorylation. *Biochemical Society Transactions*, *35*(Pt 5), 1064–1068. https://doi.org/10.1042/BST0351064

Moreno, H., Vega-Saenz de Miera, E., Nadal, M. S., Amarillo, Y., & Rudy, B. (2001). Modulation of Kv3 potassium channels expressed in CHO cells by a nitric oxide-activated phosphatase. *The Journal of Physiology*, *530* (Pt 3), 345–358. https://doi.org/10.1111/j.1469-7793.2001.0345k.x

O'Leary, T., van Rossum, M. C., & Wyllie, D. J. (2010). Homeostasis of intrinsic excitability in hippocampal neurones: Dynamics and mechanism of the response to chronic depolarization. *The Journal of Physiology*, *588*(Pt 1), 157–170. https://doi.org/10.1113/jphysiol.2009.181024

Ooi, L., Gigout, S., Pettinger, L., & Gamper, N. (2013). Triple cysteine module within M-type K+ channels mediates reciprocal channel modulation by nitric oxide and reactive oxygen species. *The Journal of Neuroscience*, *33* (14), 6041–6046. https://doi.org/10.1523/JNEUROSCI.4275-12.2013

Palacio, S., Chevaleyre, V., Brann, D. H., Murray, K. D., Piskorowski, R. A., & Trimmer, J. S. (2017). Heterogeneity in Kv2 channel expression shapes action potential characteristics and firing patterns in CA1 versus CA2 hippocampal pyramidal neurons. *eNeuro*, *4*(4), ENEURO.0267–ENEU17.2017. https://doi.org/10.1523/ENEURO.0267-17.2017

Philippides, A., Ott, S. R., Husbands, P., Lovick, T. A., & O'Shea, M. (2005). Modeling cooperative volume signaling in a plexus of nitric-oxide-synthase-expressing neurons. *The Journal of Neuroscience*, *25*(28), 6520–6532. https://doi.org/10.1523/JNEUROSCI.1264-05.2005

Pigott, B. M., & Garthwaite, J. (2016). Nitric oxide is required for L-type Ca (2+) channel-dependent long-term potentiation in the hippocampus. *Frontiers in Synaptic Neuroscience*, *8*, 17. https://doi.org/10.3389/fnsyn.2016.00017

Pires da Silva, M., de Almeida Moraes, D. J., Mecawi, A. S., Rodrigues, J. A., & Varanda, W. A. (2016). Nitric oxide modulates HCN channels in magnocellular neurons of the supraoptic nucleus of rats by an S-nitrosylation-dependent mechanism. *The Journal of Neuroscience*, *36*(44), 11320–11330. https://doi.org/10.1523/JNEUROSCI.1588-16.2016

Renganathan, M., Cummins, T. R., & Waxman, S. G. (2001). Contribution of Na(v)1.8 sodium channels to action potential electrogenesis in DRG neurons. *Journal of Neurophysiology*, *86*(2), 629–640. https://doi.org/10.1152/jn.2001.86.2.629

Renganathan, M., Cummins, T. R., & Waxman, S. G. (2002). Nitric oxide blocks fast, slow, and persistent Na+ channels in C-type DRG neurons by S-nitrosylation. *Journal of Neurophysiology*, *87*(2), 761–775. https://doi.org/10.1152/jn.00369.2001

Ribeiro, M. A., Cabral, H. O., & Costa, P. F. (2007). Modulatory effect of NO on sodium currents in a neuroblastoma cell line: Aspects of cell specificity. *Neuroscience Research*, *58*(4), 361–370. https://doi.org/10.1016/j.neures.2007.04.007

Robinson, S. W., Bourgognon, J. M., Spiers, J. G., Breda, C., Campesan, S., Butcher, A., Mallucci, G. R., Dinsdale, D., Morone, N., Mistry, R., Smith, T. M., Guerra-Martin, M., Challiss, R. A. J., Giorgini, F., & Steinert, J. R. (2018). Nitric oxide-mediated posttranslational modifications control neurotransmitter release by modulating complexin farnesylation and enhancing its clamping ability. *PLoS Biology*, *16*(4), e2003611. https://doi.org/10.1371/journal.pbio.2003611

Romero, J. M., & Bizzozero, O. A. (2009). Intracellular glutathione mediates the denitrosylation of protein nitrosothiols in the rat spinal cord. *Journal of Neuroscience Research*, *87*(3), 701–709. https://doi.org/10.1002/jnr.21897

Sekerli, M., del Negro, C. A., Lee, R. H., & Butera, R. J. (2004). Estimating action potential thresholds from neuronal time-series: New metrics and evaluation of methodologies. *IEEE Transactions on Biomedical Engineering*, *51*(9), 1665–1672. https://doi.org/10.1109/TBME.2004.827531

Sole, L., Wagnon, J. L., & Tamkun, M. M. (2020). Functional analysis of three Nav1.6 mutations causing early infantile epileptic encephalopathy. *Biochimica et Biophysica Acta - Molecular Basis of Disease*, *1866*(12), 165959. https://doi.org/10.1016/j.bbadis.2020.165959

Song, D., Wang, D., Yang, Q., Yan, T., Wang, Z., Yan, Y., Zhao, J., Xie, Z., Liu, Y., Ke, Z., Qazi, T. J., Li, Y., Wu, Y., Shi, Q., Lang, Y., Zhang, H., Huang, T., Wang, C., Quan, Z., & Qing, H. (2020). The lateralization of left hippocampal CA3 during the retrieval of spatial working memory. *Nature Communications*, *11*(1), 2901. https://doi.org/10.1038/s41467-020-16698-4

Steinert, J. R., Chernova, T., & Forsythe, I. D. (2010). Nitric oxide signaling in brain function, dysfunction, and dementia. *The Neuroscientist*, *16*(4), 435–452. https://doi.org/10.1177/1073858410366481

Steinert, J. R., Kopp-Scheinpflug, C., Baker, C., Challiss, R. A., Mistry, R., Haustein, M. D., … Forsythe, I. D. (2008). Nitric oxide is a volume transmitter regulating postsynaptic excitability at a glutamatergic synapse. *Neuron*, *60*(4), 642–656. https://doi.org/10.1016/j.neuron.2008.08.025

Steinert, J. R., Postlethwaite, M., Jordan, M. D., Chernova, T., Robinson, S. W., & Forsythe, I. D. (2010). NMDAR-mediated EPSCs are maintained and accelerate in time course during maturation of mouse and rat auditory brainstem in vitro. *The Journal of Physiology*, *588*(Pt 3), 447–463. https://doi.org/10.1113/jphysiol.2009.184317

Steinert, J. R., Robinson, S. W., Tong, H., Haustein, M. D., Kopp-Scheinpflug, C., & Forsythe, I. D. (2011). Nitric oxide is an activity-dependent regulator of target neuron intrinsic excitability. *Neuron*, *71*(2), 291–305. https://doi.org/10.1016/j.neuron.2011.05.037

Stomberski, C. T., Hess, D. T., & Stamler, J. S. (2019). Protein S-nitrosylation: Determinants of specificity and enzymatic regulation of S-nitrosothiol-based signaling. *Antioxidants & Redox Signaling*, *30*(10), 1331–1351. https://doi.org/10.1089/ars.2017.7403

Tozer, A. J., Forsythe, I. D., & Steinert, J. R. (2012). Nitric oxide signalling augments neuronal voltage-gated L-type (Ca(v)1) and P/q-type (Ca(v)2.1) channels in the mouse medial nucleus of the trapezoid body. *PLoS One*, *7*(2), e32256. https://doi.org/10.1371/journal.pone.0032256

Tricoire, L., Pelkey, K. A., Daw, M. I., Sousa, V. H., Miyoshi, G., Jeffries, B., Cauli, B., Fishell, G., & McBain, C. J. (2010). Common origins of hippocampal Ivy and nitric oxide synthase expressing neurogliaform cells. *The Journal of Neuroscience*, *30*(6), 2165–2176. https://doi.org/10.1523/JNEUROSCI.5123-09.2010

Trimmer, J. S. (2015). Subcellular localization of K+ channels in mammalian brain neurons: Remarkable precision in the midst of extraordinary complexity. *Neuron*, *85*(2), 238–256. https://doi.org/10.1016/j.neuron.2014.12.042

Turrigiano, G. G. (1999). Homeostatic plasticity in neuronal networks: The more things change, the more they stay the same. *Trends in Neurosciences*, *22*(5), 221–227. https://doi.org/10.1016/s0166-2236(98)01341-1

Westenbroek, R. E., Merrick, D. K., & Catterall, W. A. (1989). Differential subcellular localization of the RI and RII Na+ channel subtypes in central neurons. *Neuron*, *3*(6), 695–704. https://doi.org/10.1016/0896-6273(89)90238-9

Williams, S. R., & Mitchell, S. J. (2008). Direct measurement of somatic voltage clamp errors in central neurons. *Nature Neuroscience*, *11*(7), 790–798. https://doi.org/10.1038/nn.2137

Wood, K. C., Batchelor, A. M., Bartus, K., Harris, K. L., Garthwaite, G., Vernon, J., & Garthwaite, J. (2011). Picomolar nitric oxide signals from central neurons recorded using ultrasensitive detector cells. *The Journal of Biological Chemistry*, *286*(50), 43172–43181. https://doi.org/10.1074/jbc.M111.289777

Wu, C. C., Ko, F. N., Kuo, S. C., Lee, F. Y., & Teng, C. M. (1995). YC-1 inhibited human platelet aggregation through NO-independent activation of soluble guanylate cyclase. *British Journal of Pharmacology*, *116*(3), 1973–1978. https://doi.org/10.1111/j.1476-5381.1995.tb16400.x

Zemankovics, R., Kali, S., Paulsen, O., Freund, T. F., & Hajos, N. (2010). Differences in subthreshold resonance of hippocampal pyramidal cells and interneurons: The role of h-current and passive membrane characteristics. *The Journal of Physiology*, *588*(Pt 12), 2109–2132. https://doi.org/10.1113/jphysiol.2009.185975

Zhong, L. R., Estes, S., Artinian, L., & Rehder, V. (2013). Nitric oxide regulates neuronal activity via calcium-activated potassium channels. *PLoS One*, *8*(11), e78727. https://doi.org/10.1371/journal.pone.0078727

Zhong, L. R., Estes, S., Artinian, L., & Rehder, V. (2015). Cell-specific regulation of neuronal activity by endogenous production of nitric oxide. *The European Journal of Neuroscience*, *41*(8), 1013–1024. https://doi.org/10.1111/ejn.12875

How to cite this article: Scheiblich, H., & Steinert, J. R. (2021). Nitrergic modulation of neuronal excitability in the mouse hippocampus is mediated via regulation of Kv2 and voltage-gated sodium channels. *Hippocampus*, *31*(9), 1020–1038. https://doi.org/10.1002/hipo.23366